frontiers in Cellular and Infection Microbiology

ORIGINAL RESEARCH
published: 14 May 2018
doi: 10.3389/fcimb.2018.00146

Epithelial Keratins Modulate cMet Expression and Signaling and Promote InlB-Mediated *Listeria monocytogenes* Infection of HeLa Cells

Rui Cruz[1,2,3], *Isabel Pereira-Castro*[1,4], *Maria T. Almeida*[1,2], *Alexandra Moreira*[1,3,4], *Didier Cabanes*[1,2] *and Sandra Sousa*[1,2]*

[1] Group of Molecular Microbiology, Instituto de Investigação e Inovação em Saúde, Universidade do Porto, Porto, Portugal, [2] Group of Molecular Microbiology, Institute for Molecular and Cell Biology, Porto, Portugal, [3] Instituto de Ciências Biomédicas Abel Salazar, Universidade do Porto, Porto, Portugal, [4] Gene Regulation Group, Institute for Molecular and Cell Biology, Porto, Portugal

The host cytoskeleton is a major target for bacterial pathogens during infection. In particular, pathogens usurp the actin cytoskeleton function to strongly adhere to the host cell surface, to induce plasma membrane remodeling allowing invasion and to spread from cell to cell and disseminate to the whole organism. Keratins are cytoskeletal proteins that are the major components of intermediate filaments in epithelial cells however, their role in bacterial infection has been disregarded. Here we investigate the role of the major epithelial keratins, keratins 8 and 18 (K8 and K18), in the cellular infection by *Listeria monocytogenes*. We found that K8 and K18 are required for successful InlB/cMet-dependent *L. monocytogenes* infection, but are dispensable for InlA/E-cadherin-mediated invasion. Both K8 and K18 accumulate at InlB-mediated internalization sites following actin recruitment and modulate actin dynamics at those sites. We also reveal the key role of K8 and K18 in HGF-induced signaling which occurs downstream the activation of cMet. Strikingly, we show here that K18, and at a less extent K8, controls the expression of cMet and other surface receptors such TfR and integrin β1, by promoting the stability of their corresponding transcripts. Together, our results reveal novel functions for major epithelial keratins in the modulation of actin dynamics at the bacterial entry sites and in the control of surface receptors mRNA stability and expression.

Keywords: intermediate filaments, keratins, cMet signaling, *Listeria monocytogenes*, cellular infection, mRNA stability, gene expression

OPEN ACCESS

Edited by:
Stephanie M. Seveau, The Ohio State University, United States

Reviewed by:
Olivier Disson, Institut Pasteur, France
Sunil D. Saroj, Symbiosis International University, India

***Correspondence:**
Sandra Sousa
srsousa@ibmc.up.pt

Received: *04 January 2018*
Accepted: *20 April 2018*
Published: *14 May 2018*

Citation:
Cruz R, Pereira-Castro I, Almeida MT, Moreira A, Cabanes D and Sousa S (2018) Epithelial Keratins Modulate cMet Expression and Signaling and Promote InlB-Mediated Listeria monocytogenes Infection of HeLa Cells. Front. Cell. Infect. Microbiol. 8:146. doi: 10.3389/fcimb.2018.00146

INTRODUCTION

Intracellular pathogens exploit the host machinery to promote and establish infection. The host cytoskeleton is one of the preferential targets of pathogens and plays essential roles in cellular infection (Carabeo, 2011; Haglund and Welch, 2011; de Souza Santos and Orth, 2015). The role of host actin cytoskeleton in bacterial pathogenesis is by far the most documented (Colonne et al., 2016). Actin filaments and their polymerization machinery are hijacked by several human

pathogens at different stages of the infection process. In particular subversion of actin is critical for: (1) stable adhesion of pathogenic *Escherichia coli* (EPEC and EHEC) to the host cell surface, through the formation of actin-rich pedestals (Goosney et al., 2000; Gruenheid et al., 2001; Stradal and Costa, 2017); (2) invasion of epithelial cells by a variety of intracellular bacteria such as *Salmonella typhimurium*, *Shigella flexneri,* and *Listeria monocytogenes* which induce actin cytoskeleton rearrangements and host membrane remodeling (Bierne et al., 2005; Sousa et al., 2007; de Souza Santos and Orth, 2015; Valencia-Gallardo et al., 2015; Rolhion and Cossart, 2017); and 3) intracellular movement of cytosolic pathogens such as *S. flexneri*, *Rickettsia conorii,* and *L. monocytogenes* which are able to elicit the formation of actin comet tails to promote cell-to-cell spread (Bernardini et al., 1989; Mounier et al., 1990; Welch et al., 1997; Egile et al., 1999; Heinzen et al., 1999; Czuczman et al., 2014; Kuehl et al., 2015).

In contrast to actin, the role of intermediate filaments (IFs), in particular keratins, during bacterial infection is poorly characterized. IFs are also part of the host cytoskeleton and include a large group of proteins that share structural features and form apolar 10 nM wide fibrous filaments (Goldman et al., 2012). Keratins are the largest subfamily of IFs, mainly expressed in the cytoplasm of epithelial cells and their expression profile is regulated in a tissue and differentiation dependent manner (Loschke et al., 2015). Type I and type II keratins form heterodimers and organize into filaments that ensure structural integrity of epithelia and confers mechanical resilience to stress (Haines and Lane, 2012). In simple epithelial cells, Keratin 8 (K8) and Keratin 18 (K18) are the most common keratin pair (Moll et al., 2008). Besides their biomechanical functions, several studies point keratins as important players in regulatory mechanisms defining health and disease (Pan et al., 2012). K8 and K18 participate in cell cycle regulation by associating with and modulating the distribution of 14-3-3 adaptor proteins (Eriksson et al., 2009). K17 was also reported to interact with 14-3-3 proteins modulating protein synthesis by interfering with mTOR signaling (Kim et al., 2006). Additionally, mice lacking type II keratins display mislocalization of glucose transporters and downregulation of the protein synthesis machinery (Kellner and Coulombe, 2009; Vijayaraj et al., 2009). Keratin defects exacerbate cell death through increased surface expression of cell death receptors and enhanced activation of apoptotic signaling cascades (Caulin et al., 2000; He et al., 2002; Gilbert et al., 2012). Keratins are also increasingly regarded as stress proteins protecting cells and tissues from stress and injury (Toivola et al., 2010).

In the context of infection, keratins are targeted for degradation during adenovirus and *Chlamydia* infection (Chen et al., 1993; Savijoki et al., 2008), facilitate adhesion of EPEC to HeLa cells (Batchelor et al., 2004), and promote internalization of *Salmonella* (Carlson et al., 2002) and intracellular replication of *Trypanosoma cruzi* (Claser et al., 2008). Interestingly, a recent study showed that in corneal epithelial cells keratin 6a is processed into antimicrobial fragments by the ubiquitin-proteasome system to protect the host against infection (Chan et al., 2018). Despite these observations, the molecular and functional details behind keratin involvement in bacterial pathogenesis remain elusive (Geisler and Leube, 2016) and the possible role of keratins in *L. monocytogenes* infection was never addressed.

L. monocytogenes is a facultative intracellular gram-positive pathogen adapted to thrive in diverse environments (Freitag et al., 2009). In humans, it causes listeriosis, a pernicious foodborne disease (Swaminathan and Gerner-Smidt, 2007) that relies on *L. monocytogenes* capacity to enter and survive into epithelial non-phagocytic cells, through the expression of an arsenal of virulence factors (Camejo et al., 2011). *L. monocytogenes* internalization into non-phagocytic cells is mainly driven by the interaction of the bacterial surface proteins InlA and InlB, with their specific host receptors, respectively, E-cadherin and cMet (Mengaud et al., 1996; Shen et al., 2000; Pizarro-Cerdá et al., 2012). The engagement of these host receptors by the bacterial ligands triggers the activation of intracellular signaling pathways that lead to actin polymerization, myosin recruitment and further membrane remodeling, ultimately resulting in the internalization of the bacteria (Ireton et al., 1996, 1999; Bierne et al., 2001; Sousa et al., 2004, 2007; Pizarro-Cerdá et al., 2012; Almeida et al., 2015).

In this study, we assessed the role of epithelial keratins K8 and K18, during *L. monocytogenes* infection. We found that both K8 and K18 are required for successful InlB/cMet-mediated internalization of *L. monocytogenes* and HGF-induced signaling. We also observed that K8 and K18 modulate actin dynamics during InlB-driven internalization. Interestingly, we also showed here that K18, and to a lesser extent K8, control the expression of cMet and other surface receptors such as Transferrin Receptor (TfR) and Integrin β1. Indeed, K18 confers transcript stability, thus regulating post-transcriptionally the expression of such membrane proteins.

MATERIALS AND METHODS

Reagents and Antibodies

Primary antibodies used are listed in **Table 1**. Goat anti-mouse HRP or anti-rabbit HRP (P.A.R.I.S.) secondary antibodies were used at 1:2,000 for immunoblotting. For immunofluorescence, secondary antibodies goat anti-rabbit or anti-mouse Alexa Fluor 488 (Invitrogen) and goat anti-mouse or anti-rabbit Cy3 (Jackson Immunoresearch) were used at 1:300. Actin was labeled with Alexa Fluor 647 phalloidin (Invitrogen) or Phalloidin-Tetramethylrhodamine B isothiocyanate (TRITC, Sigma Aldrich). DNA was labeled with 2-(4-Amidinophenyl)-6-indolecarbamidine dihydrochloride (DAPI, Sigma Aldrich). Concanamycin A, MG132 and Actinomycin D were obtained from Sigma Aldrich. HGF was purchased from Peprotech.

Bacterial Strains and Cell Lines

L. monocytogenes EGDe strain was grown at 37°C with shaking in brain heart infusion (BHI; BD-Difco). *Listeria innocua* InlB was grown in BHI supplemented with 5 μg/ml erythromycin. *E. coli* K12-*inv* was grown at 37°C with shaking in lysogeny broth (LB) supplemented with 100 μg/ml ampicillin.

HeLa cells (ATCC CCL-2) were cultured in DMEM supplemented with glucose (4.5 g/l), L-glutamine and 10% fetal

bovine serum (FBS, Biowest). Caco-2 cells (ATCC HTB-37) were maintained in EMEM supplemented with 20% FBS, L-glutamine, sodium pyruvate and non-essential amino acids. Cells were maintained at 37°C in a 5% CO_2 atmosphere. Cell culture media and supplements were from Lonza.

Bacterial Infections

Cell infections were performed as described (Reis et al., 2010). For adhesion experiments, bacteria in exponential phase of growth were washed and inoculated at a multiplicity of infection (MOI) of 50. After 30 min, cells were washed five times with phosphate buffered saline (PBS), lysed in 0.2% Triton-X-100 and serial dilutions were plated for quantification of viable bacteria (colony forming units-CFU). For invasion assays, inoculum was prepared as above and cells were infected for 60 min, washed and incubated with medium supplemented with 20 μg/ml gentamicin for 90 min. Cells were washed, lysed with 0.2% Triton-X-100 and serial dilutions plated for CFU counting. For immunofluorescence scoring of adhered and intracellular *L. innocua*-InlB, HeLa cells were inoculated at a MOI of 50 for 30 min, washed and fixed. Before permeabilization, extracellular bacteria were labeled with a rabbit polyclonal antibody raised against *L. innocua* (R6, kindly provided by Prof Pascale Cossart, Institut Pasteur) and an appropriate secondary antibody. Cells were then permeabilized with 0.1% Triton X-100 and total bacteria were labeled with R6 and a secondary antibody coupled to a different fluorochrome. Total and extracellular bacteria were counted under the microscope. For intracellular replication assays, cells were infected with a MOI of 1 for 60 min, washed and incubated with medium complemented with 20 mg/ml gentamicin for 90 min, washed and lysed 2.5, 5, 7, 9, and 12 h after infection. Adhesion and invasion assays were performed in triplicate and repeated at least three times. Replication assays were performed twice in duplicate. For immunofluorescence experiments, cells were infected with *L. innocua* InlB (MOI of 50), washed in PBS and fixed in 3% paraformaldehyde.

TABLE 1 | List of antibodies used in this study.

Antigen	Species	Applications	References	Source
Phosphotyrosine	Mouse	IP (1:360)	4G10, 05-321	Millipore
Actin	Mouse	WB (1:5,000)	A5441	Sigma Aldrich
GAPDH	Mouse	WB (1:15,000)	sc-32233	Santa Cruz Biotechnologies
K8	Mouse	WB (1:450), IF (1:200)	sc-8020	Santa Cruz Biotechnologies
K8	Rabbit	WB (1:10,000), IF (1:400)	ab53280	Abcam
K18	Mouse	WB (1:2,000), IF (1:200)	sc-6259	Santa Cruz Biotechnologies
K18	Rabbit	WB (1:10,000), IF (1:400)	ab52948	Abcam
cMet	Rabbit	WB (1:175), IF (1:150)	Sc-10	Santa Cruz Biotechnologies
TfR	Mouse	WB (1:1500)	13-6800	Thermo
Integrin-β1	Rabbit	WB (1:1,000)	ab52971	Abcam
PI3Kp85	Rabbit	WB (1:1500)	06-195	Millipore
e-cadherin	Rabbit	WB (1:300)	sc-7870	Santa Cruz Biotechnologies
S6	Mouse	WB (1:1,600)	2317	Cell Signaling
Phospho-S6	Rabbit	WB (1:1,000)	4856	Cell Signaling
Akt	Rabbit	WB (1:1,000)	4685	Cell Signaling
P-Akt (S473)	Rabbit	WB (1:1,500)	4060	Cell Signaling

WB, Western blot; IF, immunofluorescence.

Transfection of siRNA Duplexes

HeLa cells were seeded in 24 or 6 well plates and transfected with 46 nM control siRNA-D (sc-44232, Santa Cruz Biotechnology) or with specific siRNAs for K8 or K18 depletion (oligo sequences on **Table 2**). For partial depletion, we used 13.8 nM of siRNA duplexes. Transfection was performed with HiPerFect (Qiagen) immediately after cell seeding, according to the manufacturer's instructions. Assays were performed 72 h pot-transfection. Transfection of Caco-2 cells was performed with Amaxa Cell line Nucleofector Kit T (Lonza) using program B-024 and following manufacturer's instructions.

Immunoblotting

Protein samples were diluted in Laemmli buffer containing 5% β-mercaptoethanol, resolved on SDS-PAGE gels and transferred to nitrocellulose membranes (Bio-Rad Laboratories). Membranes were blocked in 4% bovine serum albumin (BSA; Sigma Aldrich) or 5% skimmed milk dissolved in TBS-Triton (150 mM NaCl, 20 mM Tris-HCl, pH 7.4, and 0.1% Triton X-100) for 1 h. Primary antibodies were diluted in 2.5% skimmed milk or 4% BSA and incubated overnight at 4°C, incubation with HRP-conjugated secondary antibodies was performed at room temperature for 1 h. ECL (Thermo Scientific) or SuperSignal West Dura Extended Duration Substrate (Pierce) were used for detection of signal on X-ray films (Thermo Scientific) or digitally acquired in a ChemiDoc XRS+ system (Bio-Rad Laboratories).

Immunoprecipitation Assays

Per condition, 2×10^6 cells were washed twice with phosphate-buffered saline (PBS) and serum-starved for 8 h at 37°C and 5% CO_2. Then, cells were either left untreated or incubated with 150 ng/ml HGF for 5 min. Cells were then washed twice with ice-cold PBS and lysed in 300 μl of lysis buffer [1% NP-40, 50 mM Tris pH 7.5, 150 mM NaCl, 2 mM EDTA, 1 mM AEBSF, PhosSTOP (Roche Pharmaceuticals) and Complete Protease Inhibitor Cocktail (Roche Pharmaceuticals)].

TABLE 2 | Sequences of siRNA duplexes used in this study.

siRNA DUPLEXES		
Name	**Oligo Sequence (5′-3′)**	**Source**
K8	Sense: CUGGGAAGGAGGCCGCUAU Antisense: AUAGCGGCCUCCUUCCCAG	SIGMA (Sasi_Hs01_00166576)
K18	Sense: GAGAGGAGCUAGACAAGUA Antisense: UACUUGUCUAGCUCCUCUCUC	SIGMA (SASI_Hs01_00145009)

Lysates were centrifuged at 15,000 g for 10 min at 4°C and immunoprecipitated with 0.7 μg of anti-phosphotyrosine antibody (4G10) overnight at 4°C. Immune complexes were captured with 50 μl of PureProteome Protein A magnetic beads (Millipore) at 4°C and washed three times with wash buffer (0.2% NP-40, 50 mM Tris pH 7.5, 150 mM NaCl, 2 mM EDTA, 1 mM AEBSF, PhosSTOP, Complete Protease Inhibitor Cocktail). Immunoprecipitated proteins were eluted and boiled in Laemmli buffer.

Cell Surface Biotinylation Assay

Cell surface protein biotinlyation was performed using the EZ-Link Sulfo-NHS-Biotinylation kit (Thermo Scientific) as described in Martins et al. (2012) and accordingly to manufacturer's protocol. In brief, 2×10^6 cells were washed with ice cold PBS (pH 8), incubated with 2 mM Sulfo-NHS-biotin (2 h at 4°C), washed with cold 100 mM glycine in PBS (pH 7.2), harvested, and lysed in RIPA (sc-364162, Santa Cruz Biotechnology). Cell extracts (90 μg) were incubated with 50 μl of neutravidin agarose resin (Thermo Scientific) overnight at 4°C, with rotation. Resin was washed and captured biotinylated proteins were eluted with Laemmli buffer.

Immunofluorescence Microscopy

Cells were fixed in 3% paraformaldehyde (10 min), quenched with 20 mM NH_4Cl (1 h), permeabilized with 0.2% Triton X-100 (6 min), washed and blocked with 1% BSA in PBS. Antibodies were diluted in the blocking buffer. Coverslips were incubated with primary antibodies (1 h), washed in PBS, incubated with secondary antibodies, phalloidin TRITC or Alexa 647 and DAPI for 45 min, and mounted onto microscope slides with Aqua-Poly/Mount. Images were analyzed and collected with an epifluorescent Zeiss Axio Imager Z1 microscope or an Olympus BX63 microscope. When necessary, Z-stacks were deconvoluted with Huygens Professional Software (SVI, Netherlands) and projected with ImageJ software (NIH).

Ruffle Formation Assays

Cells were serum starved for 7 h, stimulated with 150 ng/ml HGF for 5 and 10 min, fixed in 3% paraformaldehyde (PFA) and processed for immunofluorescence. Cells with at least one actin rich membrane ruffle were scored as ruffle-positive, cells with no ruffles were considered ruffle-negative. Data were obtained from four independent experiments, for which at least 180 cells/condition were analyzed.

Rates of Total Protein Synthesis

Cells (2×10^6) were labeled with ^{35}S-methionine (22.5 uCi/ml, PerkinElmer) in methionine free DMEM (2 h at 37°C), washed twice with PBS and lysed in RIPA buffer. Protein samples diluted in Laemmli buffer were loaded into a 10% polyacrylamide gel and resolved by SDS-PAGE, followed by autoradiography.

Quantitative Real-Time PCR

Total RNAs were isolated using TripleXtractor (GRiSP), following manufacturer's protocol. Purified RNAs (1 μg) were reverse transcribed with iScript cDNA Synthesis Kit (Bio-Rad Laboratories). Quantitative real-time PCR (qRT-PCR) was performed in 10 μl reactions containing 5 μl iTaq Universal SYBR Green Supermix (Bio-Rad Laboratories), 1 μl of cDNA and 0.1 μl of 10 μM forward and reverse primers (**Table 3**), using the following protocol: 3 min (95°C), followed by 40 cycles of 10 s (95°C), 20 s (55.6°C), and 20 s (72°C). Each target gene was analyzed in triplicate and blank control was included for each primer pair. The comparative threshold method (ΔΔCt) was used to analyze the amplification data after normalization of the test and control sample expression values to a housekeeping reference gene (GAPDH).

TABLE 3 | Sequences of primers used in this study.

PRIMER SEQUENCES (5′-3′)	
cMet	Fw: CCCTATCAAATATGTCAACG
	Rev: TCAGAAGTGTCCTATTAAAGC
TFRC	Fw: GGAATATGGAAGGAGACT
	Rev: ATAGTGATCTGGTTCTACA
ITGB1	Fw: GCCATTATTATGATTATCCTTCT
	Rev: GTTCCTACTGCTGACTTAG
GAPDH	Fw: CCTCAAGATCATCAGCAATG
	Rev: CACGATACCAAAGTTGTCAT

mRNA Stability Assays

Cells were incubated with Actinomycin D (5 μg/ml) for 1 and 2 h to inhibit *de novo* RNA synthesis. Cells were harvested and RNAs isolated, reverse transcribed and analyzed by qRT-PCR. GAPDH was used as reference gene and fold changes were normalized to the untreated control. At least three independent experiments were performed for each gene of interest.

InlB-Coated Beads Assays

Purified InlB (350 μg) was covalently coupled to 200 μl of a 4% aqueous suspension of 1.0 μm carboxylated modified latex beads (Thermo Scientific), following manufacturer's instructions. To synchronize the uptake, HeLa cells were incubated with InlB-coated beads at 4°C, centrifuged (5 min at 320 g) and incubated at 37°C. Cells were washed in ice cold PBS and processed for immunofluorescence. At least 20 cells and more than 150 beads were analyzed per condition, in at least three independent experiments. To assess internalization, extracellular beads were stained with anti-InlB B4-6 antibody (Braun et al., 1999) before cell permeabilization. Samples were then analyzed in a high-throughput widefield fluorescence microscope (IN Cell Analyzer 2000, GE Healthcare). Total beads number was quantified in brightfield. Per condition, at least 500 cells and 5,000 beads were analyzed.

Statistical Analyses

Statistical analyses were performed with Prism 7 software (GraphPad) using: two-tailed unpaired Student's *t*-test for comparison of means between two samples, one-tailed *t*-test for comparisons with samples arbitrarily fixed to 100 and one-way ANOVA with Dunnett's *post-hoc* analysis to compare different

means in relation to a control sample. Differences were not considered statistically significant for $p \geq 0.05$

RESULTS

K8 and K18 Favor InlB/cMet-Mediated *L. monocytogenes* Cellular Invasion

We assessed the relevance of keratins during *L. monocytogenes* cellular infection of epithelial cell lines, which mainly express K8 and K18 (Moll et al., 2008). HeLa and Caco-2 cells were depleted for K8 and/or K18 through an siRNA approach and intracellular *L. monocytogenes* numbers were evaluated by gentamicin protection assays (Almeida et al., 2015). Numbers of intracellular bacteria were significantly decreased in K8, K18, and K8/K18-depleted HeLa cells, as compared to control cells (**Figure 1A**). In turn, in Caco-2 cells, the depletion of K8 and/or K18 had no effect on the number of intracellular bacteria (**Supplemental Figure 1**). Furthermore, K8 and/or K18 depletion in HeLa had no impact on the ability of bacteria to adhere to the cells (**Figure 1B**). The efficiency of K8 and/or K18 depletion in the different cell lines was confirmed by western blot analysis, using GAPDH as loading control (**Supplemental Figure 2**). Altogether these data indicate that K8 and K18 are required for internalization of *L. monocytogenes* in HeLa cells, but not in Caco-2 cells.

L. monocytogenes invasion of epithelial cells is mainly driven by the interaction of the bacterial surface proteins InlA and InlB with their host receptors E-cadherin and cMet, respectively (Mengaud et al., 1996; Shen et al., 2000). In HeLa cells *Listeria* internalization largely occurs through the InlB/cMet axis, while in Caco-2 cells invasion relies essentially on the InlA/E-cadherin interplay (Shen et al., 2000; Sousa et al., 2007). The observation that keratins are specifically required for *L. monocytogenes* infection of HeLa, but not Caco-2 cells suggested that K8 and K18 are particularly important for the InlB/cMet-mediated internalization pathway. To confirm this, we evaluated in K8- and/or K18-depleted HeLa cells the internalization of *L. innocua* expressing InlB (*L. innocua*-InlB), which invades non-phagocytic cells exclusively through the InlB pathway (Braun et al., 1999). Similarly to what we observed for *L. monocytogenes*, internalization of *L. innocua*-InlB was compromised in K8- and/or K18-depleted cells (**Figures 1C,D**), thus confirming that K8 and K18 are required for efficient InlB/cMet-mediated entry of *L. monocytogenes* into human epithelial cells. Finally, we found that K8 and K18 are not involved in intracellular replication of *L. monocytogenes* in HeLa cells (**Supplemental Figure 3**). Taken together, these results

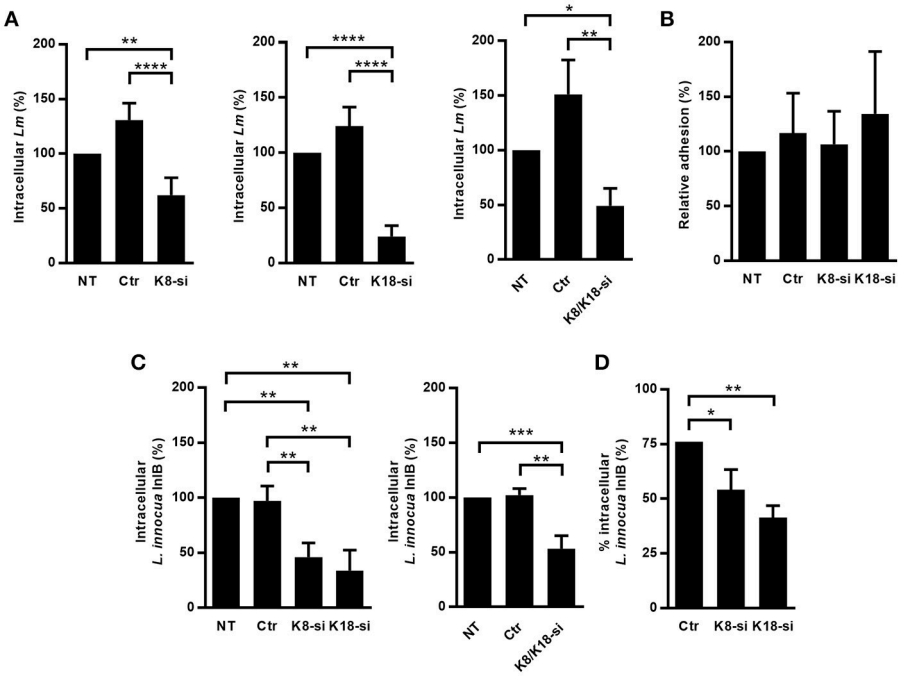

FIGURE 1 | K8 and K18 promote *Listeria* infection of HeLa cells. **(A)** Intracellular levels of *L. monocytogenes* were determined by gentamicin protection assay and CFU counting in HeLa cells left untransfected (NT) or transfected with either control (Ctr) or siRNA specifically targeting K8 (K8-si, left panel), K18 (K18-si, middle panel) and both (K8/K18-si, right panel). **(B)** Adhesion of *L. monocytogenes* was assessed in HeLa cells left unstransfected (NT) or transfected with Ctr, K8 or K18 siRNA. **(C,D)** Intracellular levels of *L. innocua* expressing InlB (*L. innocua* InlB) were determined **(C)** by gentamicin protection assays and CFU counting in HeLa cells left unstransfected (NT) or transfected with Ctr or specific siRNA targeting K8 (K8-si left panel), K18 (K18-si, left panel) and both (K8/K18-si, right panel) or by **(D)** immunofluorescence scoring of extracellular and total bacteria. Values of intracellular or adherent bacteria in NT cells were normalized to 100% and the levels of infection in the remaining conditions are expressed as relative values. Values represent the mean ± S.E. of at least three independent experiments, each done in triplicate. Statistically significant differences are indicated: $^{*}p < 0.05$, $^{**}p < 0.01$, $^{***}p < 0.001$, and $^{****}p < 0.0001$.

demonstrate that K8 and K18 play a key role in InlB/cMet-mediated internalization of *L. monocytogenes*.

K8 and K18 Accumulate at InlB-Mediated Internalization Sites

To further characterize the role of K8 and K18 in InlB-driven invasion of *Listeria*, we investigated their cellular distribution in infected cells. HeLa cells were infected with *L. innocua*-InlB, fixed and processed for immunofluorescence. K8, K18, and cMet were immunolabeled using specific antibodies, DNA was stained using DAPI and actin was detected by phalloidin staining. K8 and K18 accumulated at the vicinity of the bacteria within minutes after infection (**Figure 2A**), together with F-actin and cMet, two proteins already described to accumulate at sites of entering bacteria (Bierne et al., 2001). Quantifications of actin, K8 and K18 recruitments to the bacterial entry site were performed at different time points and are shown in **Figure 2B**. Although K8 and K18 recruitments were less frequent than actin recruitments, these observations further support the involvement of K8 and K18 in early steps of *Listeria* cellular invasion.

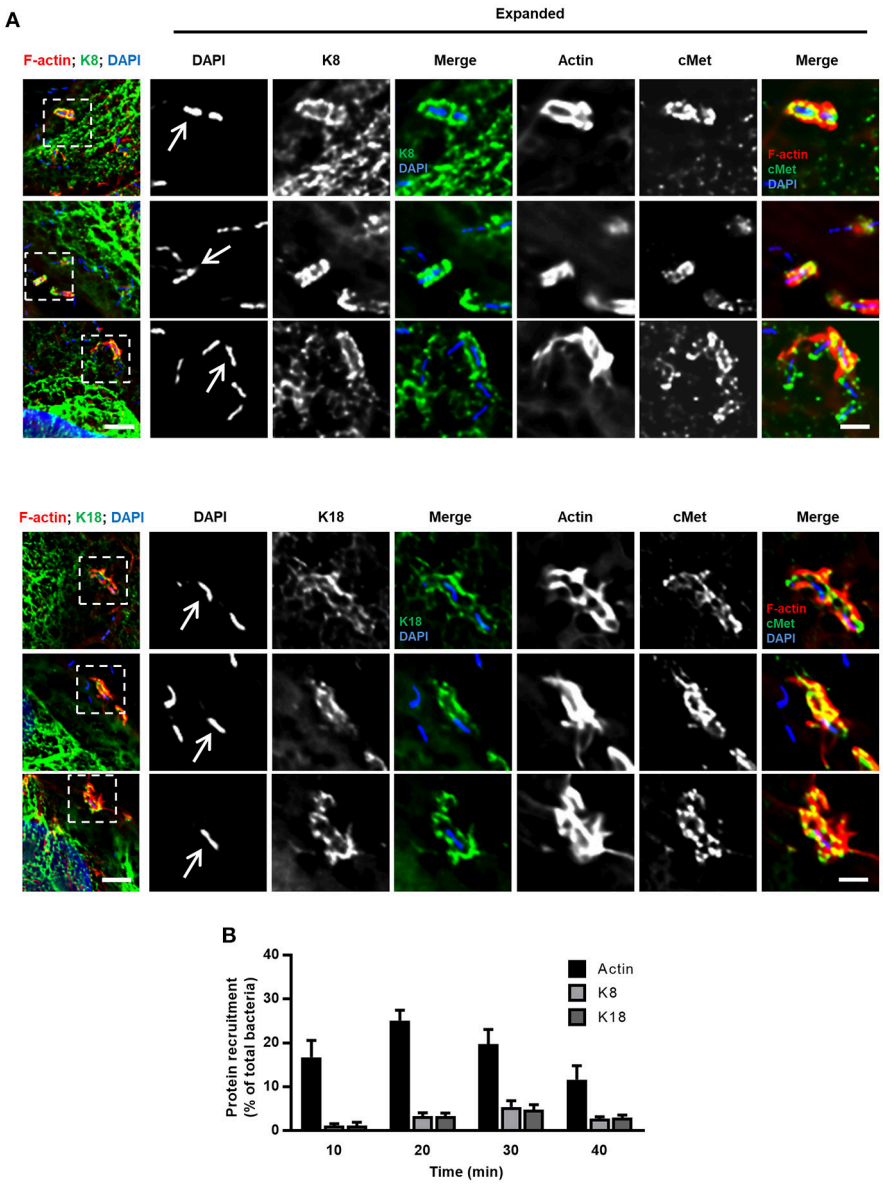

FIGURE 2 | K8 and K18 are recruited at the bacterial entry site during InlB-mediated cellular invasion. **(A)** Representative widefield microscopy stack projections of HeLa cells incubated with *L. innocua* InlB for 5 min, fixed and immunostained for cMet (green) and for K8 (upper panels, green) or K18 (lower panels, green). F-actin was stained with phalloidin (red), DNA with DAPI (blue). Scale bar, 5 μm. Arrows indicate bacteria that display accumulation of K8, K18, cMet, and F-actin at their vicinity. Insets show high-magnification images. Scale bar, 2 μm. **(B)** Quantification of K8, K18, and actin recruitments to the entry site of *L. innocua* InlB. Results are expressed as the percentage of total number of bacteria associated to cells. Values are the mean ± S.E. of at least three independent experiments.

K8 and K18 Modulate Actin Dynamics at InlB-Mediated Entry Sites

The entry process of *L. monocytogenes* into epithelial cells is a dynamic process that engages actin rearrangements and membrane remodeling (Pizarro-Cerdá et al., 2012). To gain better understanding of the dynamics of keratin recruitment to the sites of internalization and to further dissect the role of keratins in such process, we used InlB-coated beads whose entry mimics the InlB/cMet-mediated *L. monocytogenes* internalization (Braun et al., 1999; Pizarro-Cerdá et al., 2002). HeLa cells were incubated with InlB-coated beads for different periods of time and processed for immunofluorescence analysis. As we reported for *L. innocua*-InlB (**Figure 2**), K8 and K18 accumulated around entering InlB-coated beads (**Figure 3A**). We quantified the percentage of InlB-coated beads associated with actin, and K8 and K18 recruitments at different incubation time points (**Figure 3B**). As previously reported (Bierne et al., 2001), actin filaments rapidly accumulate at the vicinity of InlB-coated beads. Actin recruitment peaked at 15 min, with 60% of the beads associated to actin filaments, and promptly decreased afterwards. In turn, K8 and K18 recruitments to the vicinity of InlB-coated beads appeared later, being maximum at 30 min and sustained for longer incubation periods (**Figure 3B**). These data indicate that actin and keratin recruitments are sequential events during the internalization process of beads. To assess the potential role of K8/K18 on actin dynamics, HeLa cells depleted for K8 or K18 were incubated with InlB-coated beads for different periods of time, processed for immunofluorescence and actin recruitments around beads were quantified. In accordance to our results in **Figure 3B**, in control cells actin rings surrounding InlB-coated beads peaked at 15 min after incubation to then rapidly decrease at later time points (**Figure 3C**). In K8- and K18-depleted cells, while the percentage of InlB-coated beads associated to actin rings were equivalent to those of control cells at 15 min, they remain significantly higher at 30 min (**Figure 3C**). In cells partially depleted for K8 or K18 the levels of InlB-beads associated to actin rings are intermediate between those of control and more robustly depleted cells (**Supplemental Figure 4**). Thus, the persistence of polymerized actin around entering InlB-beads depends on the expression levels of K8 and K18. Low K8 and K18 expression increases the time during which polymerized actin associates with InlB-entering beads. These data strongly suggest a role for K8/K18 in the regulation of actin depolymerization necessary for the effective internalization of particles (Bierne et al., 2001).

K8 and K18 Control HGF/cMet-Mediated Signaling

The data obtained in the context of *Listeria* InlB/cMet-mediated internalization suggested a role for K8/K18 in cMet downstream signaling. It was previously demonstrated that InlB triggers cMet similarly to its natural ligand, the hepatocyte growth factor (HGF) (Li et al., 2005). Indeed, both HGF and InlB bind and activate cMet, and share common downstream signaling cascades that trigger MAPK and PI3-kinase pathways to promote either cell migration and proliferation or bacterial internalization (Ireton et al., 1996; Tang et al., 1998; Shen et al., 2000; Copp et al., 2003). To assess the potential role of K8/K18 in the HGF/cMet signaling pathway, we analyzed and quantified the formation of HGF-induced membrane ruffles in control, K8- and K18-depleted cells. Cells were stimulated with HGF for different time periods, fixed and processed for immunofluorescence. Membrane ruffles were detected through actin staining, which locally accumulate at the cortex of the cells undergoing ruffling (**Figure 4A**). Cells with at least one actin-rich membrane ruffle were scored as positive. While in control cells, HGF stimulation quickly induced the formation of actin rich ruffles that peaked at 5 min, in K8-and K18-depleted cells ruffle formation was compromised even at longer time points (**Figure 4B**). These data indicate that K8 and K18 also play a role in HGF-induced cMet signaling.

To further dissect the role of K8/K18 in cMet downstream signaling, we assessed HGF-dependent activation of PI3-kinase (PI3K) in control, K8 and K18-depleted cells. Serum-starved cells were incubated with HGF for 5 min, washed and lysed. Cell lysates were subjected to anti-phosphotyrosine immunoprecipitation and revealed for the PI3K p85 subunit. Western blots of phosphotyrosine enriched protein fractions showed decreased levels of the PI3K p85 subunit in K8/K18-depleted cells (**Figure 4C**), indicating an impaired association of PI3K with tyrosine phosphorylated proteins in absence of keratins and suggesting a defect in PI3K activation. In addition, K18-depleted cell lysates were directly subjected to immunoblot analysis to detect phosphorylation of Akt on serine 473 (P-Akt, S473), a direct downstream target of PI3K activity (Basar et al., 2005; Vanhaesebroeck et al., 2012; Gessain et al., 2015). As expected, in control cells HGF stimulation induced robust phosphorylation of Akt, which is extensively compromised in K18-depleted cells (**Figures 4D,E**). Together, these results demonstrate that K18, and to a lesser extent K8, are important players in the cMet-mediated signaling cascade and suggest that K8/K18 are involved upstream the activation of PI3K.

cMet Expression Is Dependent on K8 and K18

To identify the precise role of K8/K18 in cMet-mediated signaling upstream PI3K activation, we assessed the expression and activation levels of cMet. Indeed, both InlB-mediated *L. monocytogenes* internalization and the formation of HGF-triggered membrane ruffles rely on the surface expression and auto-phosphorylation of cMet on tyrosine residues (Shen et al., 2000). Interestingly, K8 and K18 were reported as modulators of the expression and/or localization of surface proteins such as the apoptotic receptor Fas, the chloride transporter DRA and the cystic fibrosis transmembrane conductance regulator (CFTR) (Gilbert et al., 2001; Duan et al., 2012; Asghar et al., 2016). Thus, this raises the possibility that keratins may also modulate cMet expression and/or activity. We evaluated the levels of total cMet expression and activation upon HGF stimulation in whole cell lysates of control, K8- and K18-depleted cells. Surprisingly, we observed that cells depleted for K8 or K18 displayed reduced levels of total cMet (**Figures 5A–C**). Nevertheless, upon HGF

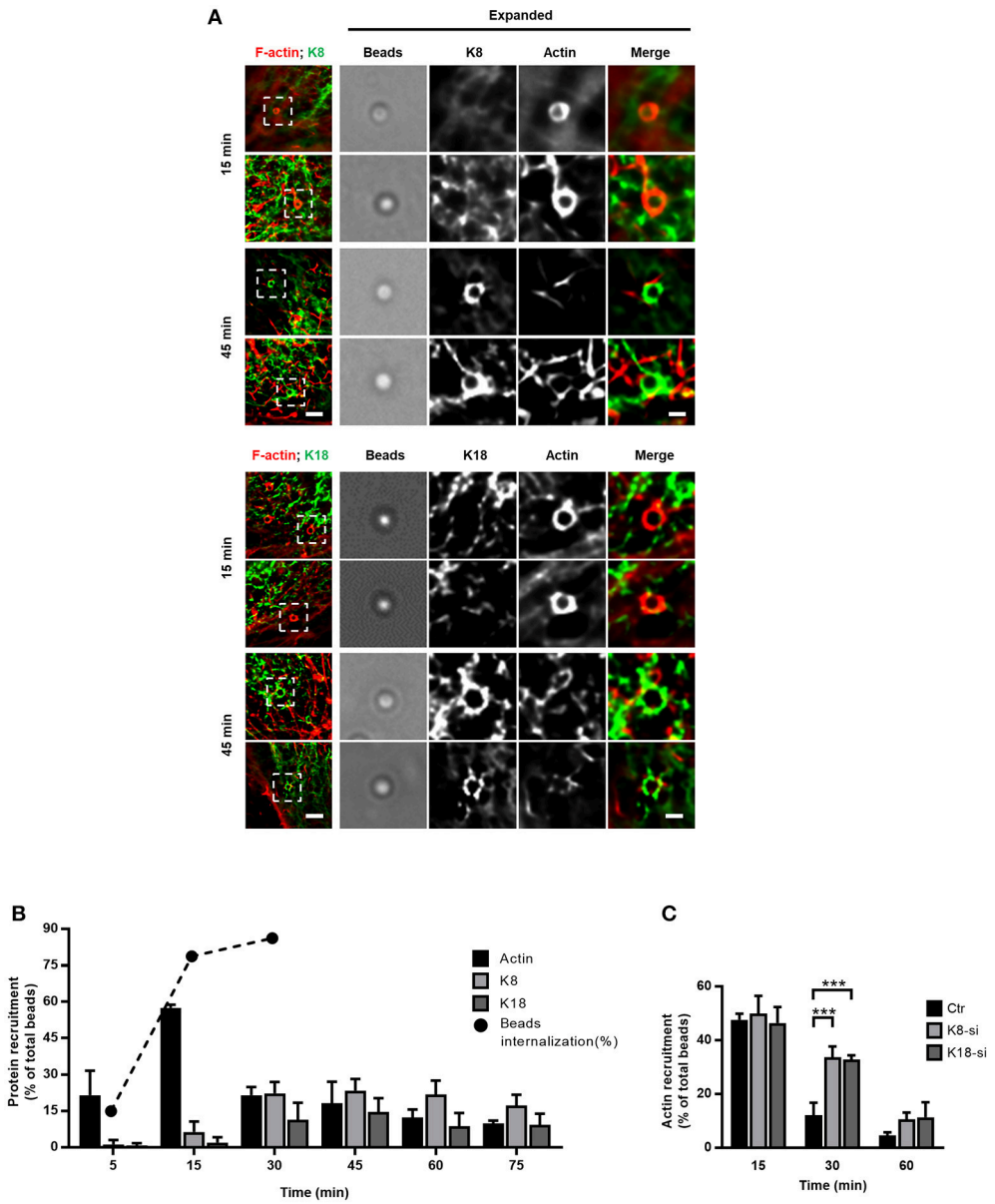

FIGURE 3 | K8 and K18 assist actin depolymerization during later stages of internalization. **(A,B)** Kinetic analysis of actin, K8 and K18 recruitments during internalization of InlB-coated latex beads. **(A)** Stack projections of widefield microscopy images of HeLa cells incubated with InlB-coated latex beads for different periods of time, fixed, immunostained for K8 or K18 (green) and labeled for F-actin with TRITC-phalloidin (red). Scale bar, 3 μm. Insets show high-magnification images. Scale bar, 1 μm. **(B)** Quantification of beads positive for K8, K18, or actin recruitment. Results are expressed as the percentage of particles associated with either protein in relation to the total number of particles associated to cells. The total number of beads was determined in brightfield. Values are the mean ± S.E. of at least three independent experiments. For determination of beads internalization, extracellular beads were stained with anti-InlB before cell permeabilization and total beads number quantified in brightfield. Values are shown in percentage and are representative of two independent experiments. **(C)** Quantification of InlB-coated latex beads associated to polymerized actin in HeLa cells transfected with control (Ctr) or specific siRNA targeting K8 (K8-si) or K18 (K18-si). Cells were incubated with InlB-coated latex beads for 15, 30, and 60 min, fixed and stained for F-actin. Beads displaying actin recruitment were considered recruitment-positive. The total number of beads associated to cells was determined in brightfield. Values represent the mean ± S.E. of at least three independent experiments. Statistically significant differences are indicated: $^{***}p < 0.001$.

stimulation cMet activation, as measured by phosphotyrosine immunoprecipitation assays, was detected at variable extents in those cells (**Figure 5A**). To determine if the low levels of total cMet expression observed in K8- and K18-depleted cells also result in a reduction of cell surface associated cMet, we specifically analyzed and quantified cell surface expression of cMet by performing biotinylation assays. Surface proteins of control, K8- and K18-depleted cells were labeled using a

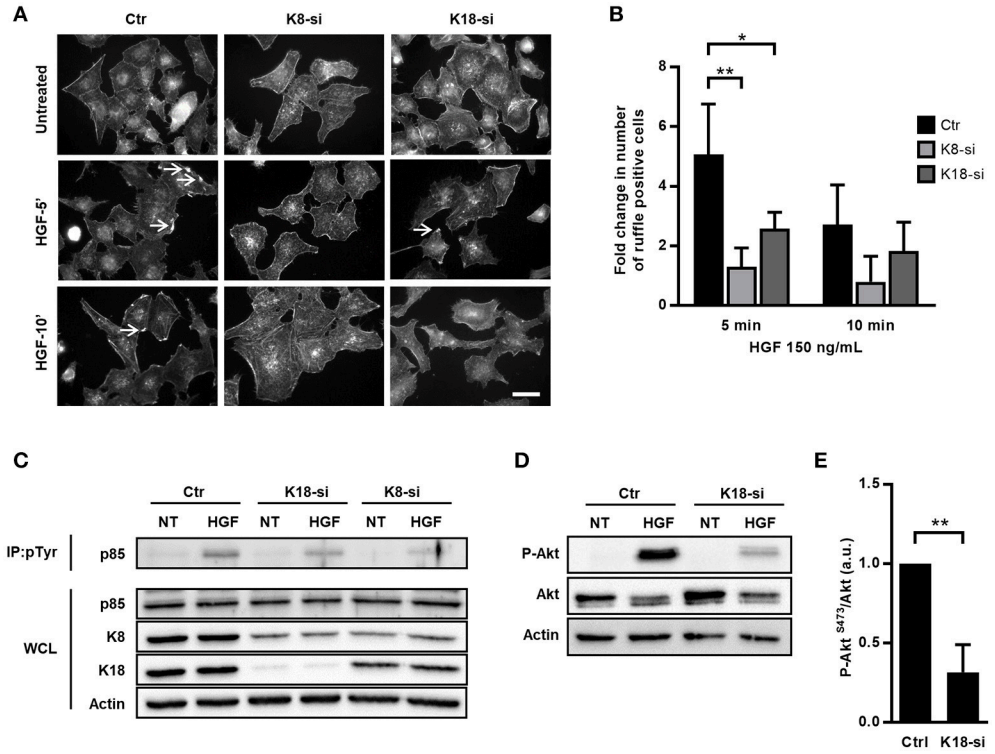

FIGURE 4 | K8 and K18 mediate cMet downstream signaling. **(A)** Immunofluorescence microscopy images of control (Ctr), K8 (K8-si), or K18 (K18-si) depleted HeLa cells left untreated or incubated with HGF (150 ng/ml) for 5 and 10 min (HGF-5′ and HGF-10′). Cells were fixed and stained for actin with TRITC-phalloidin. Images show the actin-rich membrane ruffles (arrows) induced by the HGF stimulation of cMet. Scale bar, 20 μm. **(B)** Quantification of actin-rich membrane ruffles in Ctr, K8- and K18-depleted cells. Cells without ruffles were considered ruffle-negative, whereas cells with at least one actin-rich membrane ruffle were scored as ruffle-positive. Values result from four independent experiments and are expressed as fold change with respect to untreated control cells. **(C)** Ctr, K8 and K18-depleted HeLa cells were incubated with 150 ng/ml HGF for 5 min, washed and lysed. Tyrosine phosphorylated proteins were immunoprecipitated (IP: pTyr) from whole cell lysates (WCL) and p85 was detected by immunoblot (p85) in IP fractions and WCL. Detection of actin was used as loading control. **(D)** Immunoblot to detect P-Akt (S473), total Akt and actin on total extracts of Ctr and K18-depleted HeLa cells left untreated (NT) or incubated with 150 ng/ml HGF for 5 min. **(E)** Densitometry analysis of the ratio of P-Akt (S473) over total Akt, in conditions of HGF stimulation. For control cells the value was arbitrarily fixed to 1. Values represent the mean ±S.E. of three independent experiments. Statistically significant differences are indicated: $^{*}p < 0.05$ and $^{**}p < 0.01$.

membrane-impermeable biotinylation reagent, recovered with neutravidin-coupled beads and analyzed by immunoblot. In agreement with the observed reduced levels of total cMet expression, K8 or K18 depletion resulted in decreased levels of cMet at the cell surface (**Figures 5B,C**). Altogether, these data clearly indicate that K8 and K18 control the global and surface expression of cMet, thus impacting cMet-mediated signaling events elicited by ligands such as HGF and *L. monocytogenes* InlB.

K18 Controls the Expression of Other Transmembrane Receptors

Given that K8 and K18 were already reported as modulators of expression of surface proteins (Duan et al., 2012; Asghar et al., 2016) and taking into account our data, we hypothesized that K8 and K18 may have a broad role in controlling the expression of surface receptors. To investigate this hypothesis, we assessed the impact of K8 and K18 on the expression and surface localization of transferrin receptor (TfR) and integrin β1 in HeLa cells. Immunoblot analysis of whole cell lysates and surface biotinylated fractions revealed that K18 depletion resulted in a striking decrease of total and cell surface associated levels of both TfR and integrin β1 (**Figures 6A–C**). K8 depletion lead to a mild reduction of total and surface localized TfR and had no significant effect on the expression of integrin β1 (**Figures 6A–C**). Additionally, we performed similar experiments in Caco-2 cells and observed that K18 depletion also lead to a reduction of total and surface levels of cMet, TfR, and integrin β1 (**Supplemental Figure 5**), suggesting that the mechanism through which K18 regulates the expression of these proteins is conserved in different cellular systems. Interestingly, the expression of E-cadherin is not dependent on keratins (**Supplemental Figure 4**).

To functionally assess the impact of integrin β1 downregulation induced by K18 depletion, we measured levels of internalization of *E. coli* K12 expressing the *Yersinia* invasin (K12-*inv*), which is strictly dependent on the interaction of the bacterial invasin with the host integrin β1 (Isberg and Leong, 1990). As expected, K18-depleted cells showed reduced levels of intracellular K12-*inv* (**Figure 6D**). Taken together, these results demonstrate that K18, and to a lesser extend K8, control

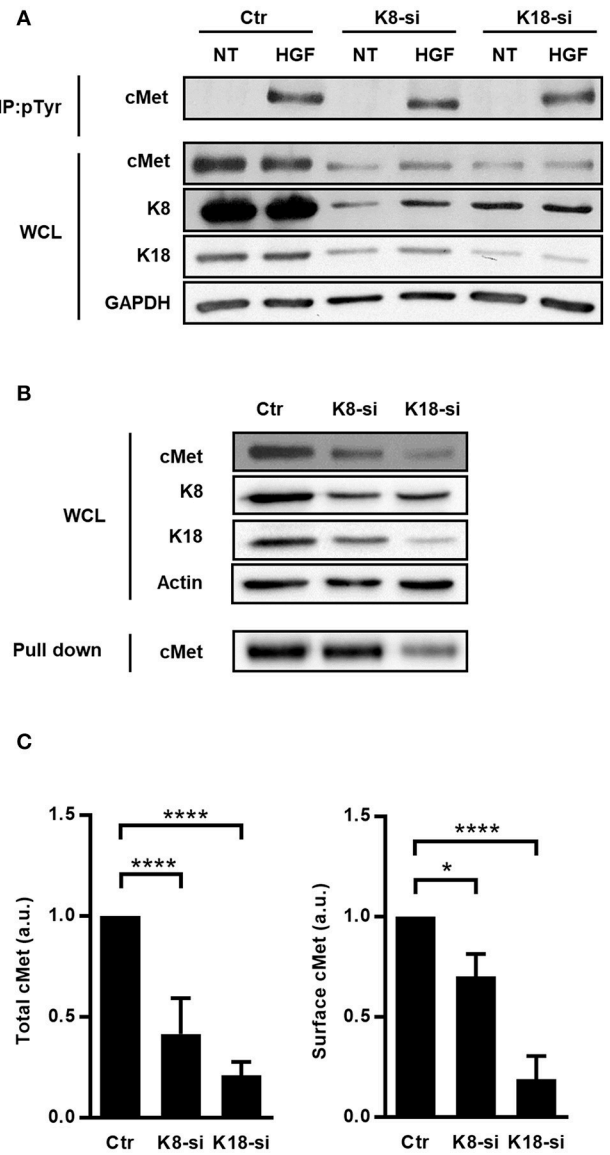

FIGURE 5 | Total expression, surface localization and activation of cMet are perturbed in cells expressing low levels of K8 and K18. **(A)** HeLa cells transfected with Ctr, K8, and K18-targeting siRNAs were left untreated (NT) or incubated with 150 ng/ml HGF for 5 min, washed and lysed. Tyrosine phosphorylated proteins were immunoprecipitated (IP: pTyr) from whole cell lysates (WCL) and cMet was analyzed by immunoblot (cMet) in IP fractions and WCL. GAPDH detection was used as loading control. **(B)** Surface exposed proteins of control (Ctr), K8- (K8-si), and K18-depleted (K18-si) HeLa cells were biotinylated and recovered from total cell extracts following neutravidin pull down assays. Biotinylated samples, corresponding to surface exposed proteins, and whole cell lysates (WCL) were immunoblotted to detect cMet, K8, K18 and actin. **(C)** Quantifications of cMet in WCL (left panel) and in biotinylated samples (right panel) from at least three independent experiments. Statistically significant differences are indicated: $^{*}p < 0.05$ and $^{****}p < 0.0001$ (a.u., arbitrary units).

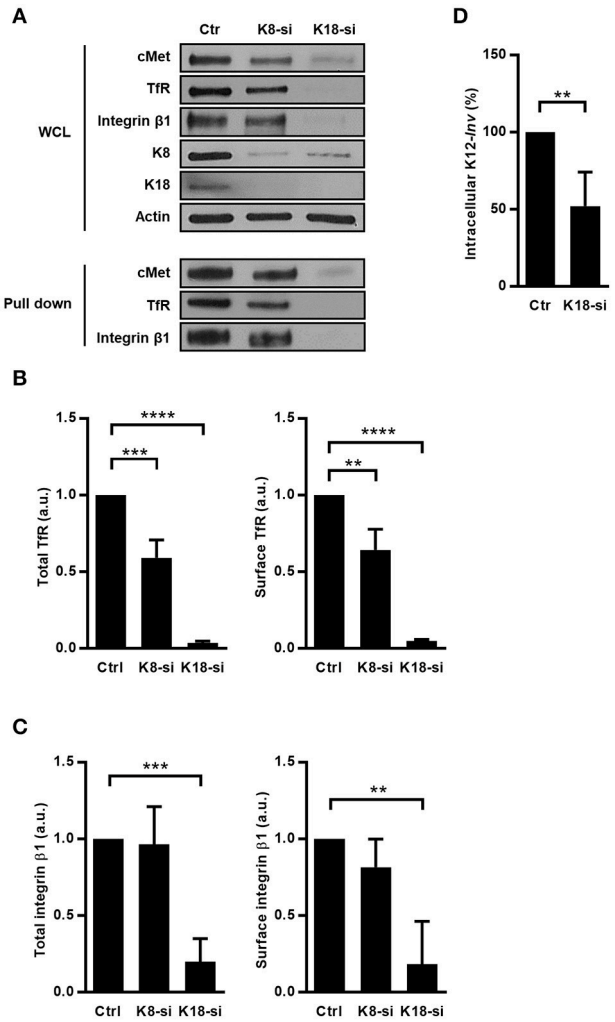

FIGURE 6 | K8 and K18 depletion perturbs expression and surface localization of transmembrane receptors. **(A)** Surface proteins of control (Ctr), K8- (K8-si), and K18-depleted (K18-si) HeLa cells were biotinylated, recovered from total cell extracts and pulled down using neutravidin beads. Biotinylated samples, which corresponds to surface exposed proteins, and whole cell lysates (WCL) were immunoblotted to detect cMet, TfR, and integrin β1, together with Actin, K8, and K18. **(B)** Quantifications of TfR in WCL (left panel) and in biotinylated samples (right panel) from at least three independent experiments. **(C)** Quantifications of integrin β1 in WCL (left panel) and in biotinylated samples (right panel) from at least three independent experiments (a.u., arbitrary units). **(D)** Functional impact of K18 in the expression of ITGB1 was assessed by gentamicin survival assay and CFU counting in K18-depleted HeLa cells (K18-si) incubated with invasive *E. coli* K12 expressing the *Y. pseudotuberculosis* invasin (K12-inv). Values of intracellular bacteria in Ctr cells were normalized to 100% and the entry levels in K18-si cells are expressed as relative values. Values are the mean ± S.E. of three independent experiments, each done in triplicate. Statistically significant differences are indicated: $^{**}p < 0.01$, $^{***}p < 0.001$, and $^{****}p < 0.0001$.

the expression of some cell surface receptors, in turn modulating signaling events taking place downstream the engagement of these receptors.

Protein Synthesis and Stability Do Not Depend on K18 Expression

The decrease of total levels of cMet, TfR, and integrin β1 observed in K18-depleted cells lead us to put forward the possibility that protein synthesis would be impaired in these cells. Indeed, K8/18

depletion was reported to lead to reduced protein synthesis in human H4 neuroglioma cells (Galarneau et al., 2007). In addition, mTOR signaling and, consequently, protein synthesis were shown to be impaired in keratinocytes lacking Keratin 17 (Kim et al., 2006). We thus assessed if mTOR signaling and global protein synthesis were compromised in K18-depleted HeLa cells, which would account for the reduced levels of cMet, TfR, and integrin β1. The ribosomal protein S6 is the target of p70S6K, a major mTOR effector (Magnuson et al., 2012), and S6 phosphorylation is thus used as a readout for mTOR activity (Biever et al., 2015; González et al., 2015). To evaluate the involvement of K18 in mTOR signaling activity, we thus analyzed the level of phosphorylated S6 in control and K18-depleted HeLa cells. S6 phosphorylation was detected in both control and K18-depleted cells (**Figure 7A**), indicating that mTOR activity is not compromised and suggesting that mTOR-dependent protein synthesis is not impaired in absence of K18. To assess the rate of bulk protein synthesis, control or K18-depleted cells were incubated with radiolabeled methionine to be incorporated into newly synthesized proteins. Total protein extracts were resolved by SDS-PAGE and labeled proteins detected by autoradiography. No major defect was detected in K18-depleted as compared to control cells (**Figure 7B**), indicating that the global initiation rate of translation is not compromised in cells lacking K18. The same samples were used in immunoblot to confirm the down-regulation of cMet, integrin β1, and TfR expression in K18-depleted cells (**Figure 7C**). These observations demonstrate that K18 does not impact significantly protein translation and *de novo* synthesis and suggest that other mechanisms should govern the K18-dependent expression of cMet, TfR and integrin β1.

Interestingly, K18 was previously reported to enhance the stability of the surface protein CFTR (Duan et al., 2012). We thus hypothesized that K18 could promote the stability of cMet, integrin β1, and TfR by minimizing their degradation. To investigate this hypothesis, control and K18-depleted HeLa cells were treated with the lysosomal inhibitor concanamycin A alone or together with the proteosomal inhibitor MG132 for different time periods. Cell extracts were immunoblotted for cMet and TfR. In both conditions tested, control and K18-depleted cells behaved similarly and no significant accumulation of cMet, integrin β1, and TfR was detected upon blockage of protein degradation (**Figure 7D**).

Altogether, these results indicate that the downregulation in the expression of cMet, TfR, and integrin β1 detected in K18-depleted cells is not due to a defect on protein synthesis or stability.

K18 Promotes Transcripts Stability

Besides translation and protein stability, regulation at the transcriptional level represents another mechanism to control protein expression. We therefore assessed if K18 depletion had an impact on transcript levels of the different receptors by qRT-PCR on mRNAs extracted from control and K18-depleted HeLa cells. *cMet*, *TfR,* and *integrin β1* mRNA levels were strongly decreased in K18-depleted cells (**Figure 8A**), with reductions ranging from 54% for *cMet* to up to 94% for *TfR*. Such reduced mRNA levels

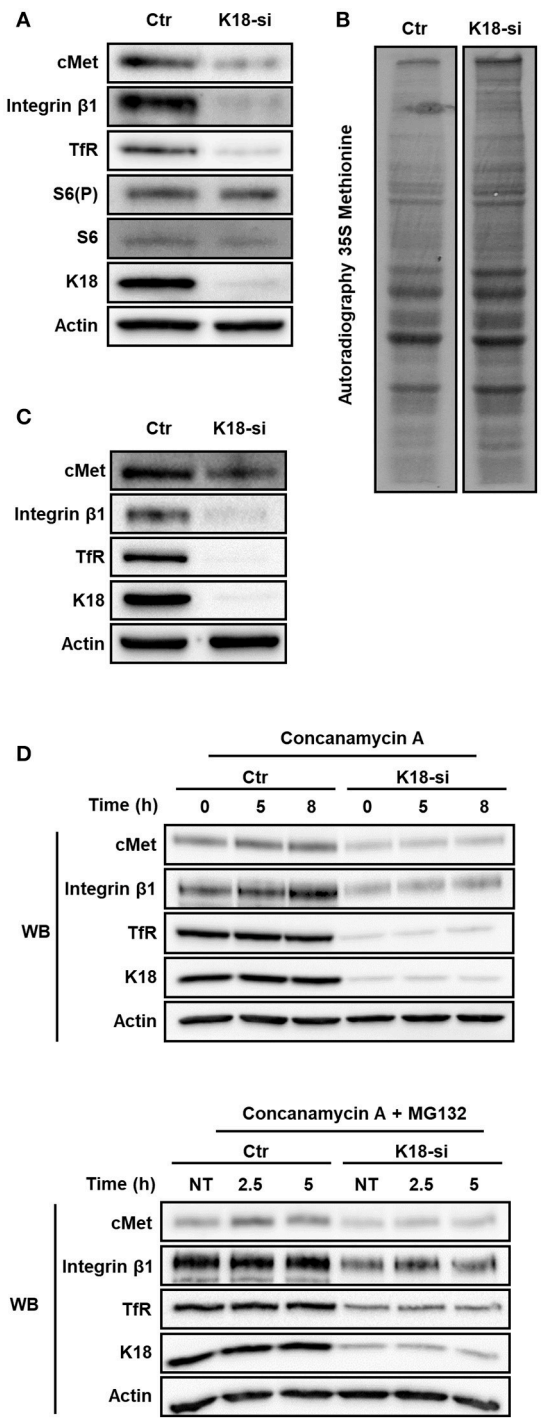

FIGURE 7 | K18 depletion does not dampen mTOR/S6K signaling, global protein translation and receptor degradation. **(A)** Activation of mTOR/S6K signaling pathway in K18 (K18-si) depleted HeLa cells was assessed by immunoblotting whole cell extracts against phosphorylated S6 (S6(P)), total S6, cMet, K18, and Actin as loading control. Immunoblot representative of three different experiments. **(B)** Rate of total protein synthesis was assessed by ^{35}S-methionine incorporation of HeLa cells transfected with control (Ctr) or K18 targeting (K18-si) siRNA. Autoradiography representative of two independent experiments. **(C)** Depletion efficiency of the samples that were

(Continued)

FIGURE 7 | used for the ^{35}S-methionine incorporation assay. **(D)** After transfection with control (Ctr) or siRNA targeting K18 (K18-si), HeLa cells were incubated with 100 nM of the lysosomal inhibitor Concanamycin A alone (*upper* panel) or together with the proteasomal inhibitor 10 μM MG132 (*lower* panel) for different periods of time. Lysates were collected and immunoblotted for cMet, TfR, integrin β1, K18, and Actin as a loading control. Immunoblots are representative of at least two independent experiments.

should therefore be responsible for the reduced cMet, TfR, and integrin β1 protein levels detected in K18-depleted cells.

Decreased steady state mRNA levels may result from a reduction in transcription or from higher instability of the mRNA (Wu and Brewer, 2012). To assess the involvement of K18 in the stability of *cMet*, *TfR,* and *integrin β1* transcripts, we measured mRNA decay in cells treated with the transcription inhibitor Actinomycin D. Control and K18-depleted HeLa cells were left untreated (0 h) or incubated with Actinomycin D for 1 and 2 h, total RNAs were extracted and analyzed by qRT-PCR. We observed that *cMet*, *TfR,* and *integrin β1* mRNAs consistently displayed a higher rate of decay in K18-depleted cells (**Figure 8B**), thus, indicating higher instability of these transcripts in cells lacking K18.

Taken together, these results demonstrate that K18 confers stability to specific transmembrane receptor mRNAs thus ensuring steady state protein levels.

DISCUSSION

Manipulation of the host cell cytoskeleton is a hallmark of the cellular infection by several human bacterial pathogens. Intermediate filaments were reported to participate in the infection process of different pathogens (Geisler and Leube, 2016), however the molecular details remain sparse. Here we demonstrate for the first time that epithelial K8 and K18 play a dual role during *L. monocytogenes* cellular infection. We found that K8 and K18 are specifically required for the successful InlB/cMet-mediated *L. monocytogenes* cell invasion by modulating the actin dynamics at the entry site and by controlling the expression of *cMet* itself. Interestingly, K18 also appeared to control the expression of other cell surface receptors, such as TfR and integrin β1, by promoting mRNA stability, thus suggesting a broader role for keratins in the regulation of gene expression.

During infection, K8 and/or K18 were previously shown to assist toxin internalization (Nava-Acosta and Navarro-Garcia, 2013), to favor intracellular pathogen replication (Claser et al., 2008) and to allow stable pathogen docking to the host cell surface (Carlson et al., 2002; Batchelor et al., 2004; Russo et al., 2016). Moreover, K8 and K18 were shown to be targeted for degradation during viral and bacterial infections (Chen et al., 1993; Seipelt et al., 2000; Savijoki et al., 2008), however the functional details of these roles remain elusive.

Keratins, as other IFs, are dynamic filament networks that interact with a multitude of proteins serving as scaffolds to organize signaling platforms and regulate different processes (Pallari and Eriksson, 2006). How K8 and K18 modulate the actin dynamics during InlB-mediated cellular invasion is still unknown. Indeed, despite several reports pointing to an interplay between actin and keratin cytoskeletons, the molecular details of such a crosstalk remain largely unidentified (Jiu et al., 2015). The link between keratins and actin is thought to be mediated by their association with linker proteins such as plectin and dystrophin (Stone et al., 2005; Karashima et al., 2012). However, other IFs such as vimentin interact directly with actin or indirectly through motors protein like myosin IIB (Esue et al., 2006; Menko et al., 2014). Actin filaments were suggested to promote the assemble of keratin network (Windoffer et al., 2006; Kölsch et al., 2009) by favoring the retrograde transports of keratin subunits. Interestingly, the formation of EGF-induced actin-rich lamellipodia was shown to be followed by the extension of the keratin network and *de novo* nucleation at the lamellipodia itself (Felkl et al., 2012). K8 and 18 were reported to interact with Grb2 and Cbl (Robertson et al., 1997; Blagoev et al., 2003; Duan et al., 2012), proteins involved in cMet signaling and InlB-dependent entry of *L. monocytogenes* (Ireton et al., 1999). In addition, keratins were found to regulate the size and organization of lipid rafts (Gilbert et al., 2012, 2016), which serve as surface membrane platforms promoting clustering of signaling molecules (Pizarro-Cerdá and Cossart, 2009), and whose integrity is required for successful InlB-mediated *L. monocytogenes* infection (Seveau et al., 2004). It is thus possible that, through interaction with adaptor proteins downstream the activation of cMet at specific places at the host plasma membrane, K8 and K18 may modulate actin dynamics at InlB entry sites. The identification of host proteins interacting with K8 and K18 specifically upon *L. monocytogenes* infection or canonical HGF-induced cMet activation should uncover the molecular details of keratin-mediated actin dynamics modulation.

Strikingly, our data highlight the role of K18 in the control of the expression of several cell surface receptors such as cMet, TfR and integrin β1. These findings are in agreement with a growing body of evidence that suggests that keratins regulate gene expression and translation (Asghar et al., 2016). Indeed, mice that lack type I or type II keratins display perturbed transcription (Kumar et al., 2015, 2016) and impaired protein expression (Vijayaraj et al., 2009). Keratin 17 was recently reported to be present in the nucleus where it interacts with the promoter regions of cytokine genes and the transcriptional regulator AIRE (Hobbs et al., 2015) thus regulating inflammatory response. Additionally, K17 regulates the shuttling between the nucleus and the cytoplasm of proteins such as hnRNP K (Chung et al., 2015), 14-3-3σ (Kim et al., 2006), and $p27^{KIP1}$ (Escobar-Hoyos et al., 2015). Nuclear accumulation of non-filamentous K18 was detected when exportin1-mediated nuclear export is inhibited (Kumeta et al., 2013), suggesting that K18, among others, may assist the nucleocytoplasmic shutting of proteins.

These observations, together with our data showing that K18 ensures the stability of certain mRNAs and thus promotes the expression of proper protein levels, tempt us to speculate that K18 may affect the shuttling of RNA-binding proteins (RBPs) from the nucleus to the cytoplasmic compartment, or the binding of specific RBPs involved in mRNA stabilization,

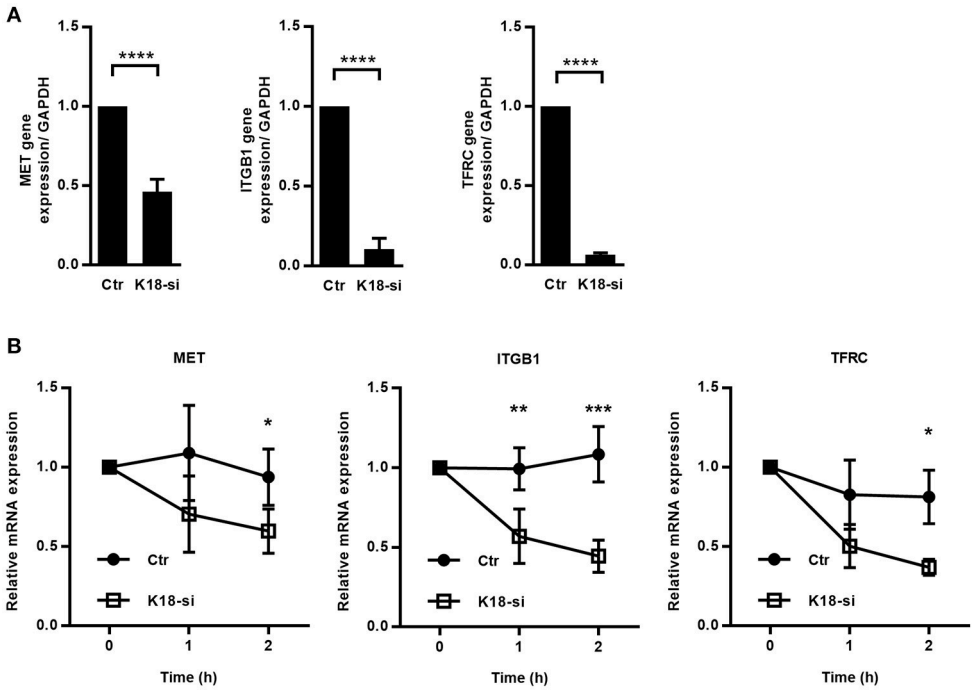

FIGURE 8 | K18 favors expression of cMet, TfR and integrin β1, by promoting transcript stability. **(A)** mRNAs were extracted from control (Ctr) and K18-depleted (K18-si) HeLa cells and qRT-PCR was performed using *GAPDH* as a housekeeping gene. Data are represented as mean ± S.E. from at least three independent experiments **(B)** Control and K18 depleted cells were left untreated or were treated with 5 μg/ml of the transcriptional inhibitor Actinomycin D for different periods of time. Transcript levels for cMet, TfR, and integrin β1 were determined by qRT-PCR. Fold changes are relative to *GAPDH* and were normalized to untreated control. Results are from at least three independent experiments. Statistically significant differences are indicated: $^{*}p < 0.05$; $^{**}p < 0.01$, $^{***}p < 0.001$, and $^{****}p < 0.0001$.

and thus impact mRNA stability. In support to this hypothesis, K18 was shown to interact with hnRNP R (Havugimana et al., 2012), an RBP that binds and stabilizes the mRNA of MHC class I genes, thus enhancing their translation (Reches et al., 2016). In addition, while searching for K18 interactors (our unpublished data), we identified by mass spectrometry the heat-shock cognate protein 70 (Hsc70), a chaperone that is able to bind and stabilize the mRNA of the proapoptotic protein Bim (Matsui et al., 2007). We also identified the PTB-associated splicing factor (PSF), an RNA and DNA binding protein that regulates transcription, alternative splicing and mRNA stability (Yarosh et al., 2015). Finally, K18 was reported to interact with the mRNA degradation machinery protein Pan2 (Bett et al., 2013), involved in the initial trimming of polyadenylated tails of mRNA, a process that favors further mRNA deadenylation and subsequent degradation (Wu and Brewer, 2012). Together with K18, knockout of K8 results in perturbed mRNA levels of multiple genes (Habtezion et al., 2011; Asghar et al., 2016; Lähdeniemi et al., 2017).

Grounded in these previous studies and our data, we propose here that K18 might modulate the stability of particular transcripts probably by interacting with specific RBPs in the cytoplasm, thus modulating the fate of the associated transcripts and ultimately controlling gene expression. The molecular understanding of the role of K18 in mRNA stability and protein expression requires further studies to identify putative RBPs interacting with K18.

AUTHOR CONTRIBUTIONS

RC, DC, and SS: conceived and designed the experiments; RC and MA: performed the experiments; RC, IP-C, AM, DC, and SS: analyzed the data; RC, DC, and SS: wrote the manuscript.

ACKNOWLEDGMENTS

This work received funding from Norte-01-0145-FEDER-000012 - Structured program on bioengineered therapies for infectious diseases and tissue regeneration, supported by Norte Portugal Regional Operational Programme (NORTE 2020), under the PORTUGAL 2020 Partnership Agreement, through the European Regional Development Fund (FEDER). Publication Fees were supported by ICBAS, University of Porto. RC received an FCT Doctoral Fellowship (SFRH/BD/90607/2012) and IP-C a FCT Post-Doctoral Fellowship (SFRH/BPD/107901/2015) through FCT/MEC co-funded by QREN and POPH (Programa Operacional Potencial Humano). SS was supported by FCT Investigator program (COMPETE, POPH, and FCT). We thank IBMC facilities for technical assistance.

SUPPLEMENTARY MATERIAL

The Supplementary Material for this article can be found online at: https://www.frontiersin.org/articles/10.3389/fcimb.2018.00146/full#supplementary-material

Supplemental Figure 1 | Keratin 8 (K8) and Keratin 18 (K18) are dispensable for *Listeria* infection of Caco-2 cells. Intracellular levels of *L. monocytogenes* were assessed by gentamicin protection assay and CFU counting in intestinal epithelial cell line Caco-2 cells that were left untransfected (NT) or transfected with control siRNA (Ctr) or with siRNAs specifically targeting K8 (K8-si, left panel), K18 (K18-si, middle panel) or both (K8/K18-si, right panel). The number of intracellular *L. monocytogenes* in NT cells was normalized to 100%, and those in siRNA-transfected cells were expressed as relative values to NT cells. Values are the mean ±S.E. of at least three independent experiments, each done in triplicate.

Supplemental Figure 2 | K8 and K18 depletion efficiency in HeLa and Caco-2 cells. Efficiency of protein knockdown in **(a)** HeLa and **(b)** Caco-2 cells was assessed by western immunoblot using GAPDH as loading control. **(c)** Immunofluorescence images of Ctr and K8- (K8-si) or K18- (K18-si) depleted HeLa cells labeled for K8 and K18. Signal intensity was quantified. The values in Ctr cells were normalized to 1, and those in K8- and K18-depleted cells were expressed as relative values. Values are the mean ± S.E. of three independent experiments.

Supplemental Figure 3 | K8 and K18 are not important for *Listeria* intracellular replication in HeLa cells. **(a)** Intracellular replication of *L. monocytogenes* in HeLa cells left untransfected (NT) or transfected with control (Ctr) or both K8 and K18 siRNA (K8/K18-si). Values represent the mean of duplicate samples from one representative experiment out of two independent experiments. **(b)** Efficiency of protein knockdown was assessed by western blot using GAPDH as loading control.

Supplemental Figure 4 | K8 and K18 assist actin depolymerization during InlB-mediated internalization. Quantification of InlB-coated latex beads associated to polymerized actin in HeLa cells transfected with control (Ctr) or different concentrations of specific siRNA targeting K8 (K8-si) or K18 (K18-si). The use of 46 nM siRNA allows the maximum keratin depletion while 13.8 nM allows partial depletion. Cells were incubated with InlB-coated latex beads for 15, 30 and 60 min, fixed and stained for F-actin. Beads displaying actin recruitment were considered recruitment-positive. The total number of beads associated to cells was determined in brightfield. Values represent the mean ±S.E. of two independent experiments.

Supplemental Figure 5 | K18 depletion perturbs expression and surface localization of transmembrane receptors in Caco-2 cells. Biotinylated surface proteins of control (Ctr) and K18-depleted (K18-si) Caco-2 cells were recovered from total cell extracts and pulled down using neutravidin beads. Biotinylated samples and whole cell lysates (WCL) were immunoblotted to detect cMet, TfR and integrin β1. **(a)** Immunoblot representative of two independent experiments. **(b)** Quantifications of E-cadherin, cMet, TfR and integrin β1 in WCL and in biotinylated samples from two independent experiments.

REFERENCES

Almeida, M. T., Mesquita, F. S., Cruz, R., Osório, H., Custódio, R., Brito, C., et al. (2015). Src-dependent tyrosine phosphorylation of non-muscle myosin heavy chain-IIA restricts *Listeria monocytogenes* cellular infection. *J. Biol. Chem.* 290, 8383–8395. doi: 10.1074/jbc.M114.591313

Asghar, M. N., Priyamvada, S., Nyström, J. H., Anbazhagan, A. N., Dudeja, P. K., and Toivola, D. M. (2016). Keratin 8 knockdown leads to loss of the chloride transporter DRA in the colon. *Am. J. Physiol.* 310, G1147–G1154. doi: 10.1152/ajpgi.00354.2015

Basar, T., Shen, Y., and Ireton, K. (2005). Redundant roles for Met docking site tyrosines and the Gab1 pleckstrin homology domain in InlB-mediated entry of *Listeria monocytogenes*. *Infect. Immun.* 73, 2061–2074. doi: 10.1128/IAI.73.4.2061-2074.2005

Batchelor, M., Guignot, J., Patel, A., Cummings, N., Cleary, J., Knutton, S., et al. (2004). Involvement of the intermediate filament protein cytokeratin-18 in actin pedestal formation during EPEC infection. *EMBO Rep.* 5, 104–110. doi: 10.1038/sj.embor.7400038

Bernardini, M. L., Mounier, J., d'Hauteville, H., Coquis-Rondon, M., and Sansonetti, P. J. (1989). Identification of icsA, a plasmid locus of *Shigella flexneri* that governs bacterial intra- and intercellular spread through interaction with F-actin. *Proc. Natl. Acad. Sci. U.S.A.* 86, 3867–3871.

Bett, J. S., Ibrahim, A. F. M., Garg, A. K., Kelly, V., Pedrioli, P., Rocha, S., et al. (2013). The P-body component USP52/PAN2 is a novel regulator of HIF1A mRNA stability. *Biochem. J.* 451, 185–194. doi: 10.1042/BJ20130026

Bierne, H., Gouin, E., Roux, P., Caroni, P., Yin, H. L., and Cossart, P. (2001). A role for cofilin and LIM kinase in Listeria-induced phagocytosis. *J. Cell Biol.* 155, 101–112. doi: 10.1083/jcb.200104037

Bierne, H., Miki, H., Innocenti, M., Scita, G., Gertler, F. B., Takenawa, T., et al. (2005). WASP-related proteins, Abi1 and Ena/VASP are required for Listeria invasion induced by the Met receptor. *J. Cell Sci.* 118, 1537–1547. doi: 10.1242/jcs.02285

Biever, A., Valjent, E., and Puighermanal, E. (2015). Ribosomal protein S6 phosphorylation in the nervous system: from regulation to function. *Front. Mol. Neurosci.* 8:75. doi: 10.3389/fnmol.2015.00075

Blagoev, B., Kratchmarova, I., Ong, S.-E., Nielsen, M., Foster, L. J., and Mann, M. (2003). A proteomics strategy to elucidate functional protein-protein interactions applied to EGF signaling. *Nat. Biotechnol.* 21, 315–318. doi: 10.1038/nbt790

Braun, L., Nato, F., Payrastre, B., Mazié, J. C., and Cossart, P. (1999). The 213-amino-acid leucine-rich repeat region of the *Listeria monocytogenes* InlB protein is sufficient for entry into mammalian cells, stimulation of PI 3-kinase and membrane ruffling. *Mol. Microbiol.* 34, 10–23. doi: 10.1046/j.1365-2958.1999.01560.x

Camejo, A., Carvalho, F., Reis, O., Leitão, E., Sousa, S., and Cabanes, D. (2011). The arsenal of virulence factors deployed by *Listeria monocytogenes* to promote its cell infection cycle. *Virulence* 2, 379–394. doi: 10.4161/viru.2.5.17703

Carabeo, R. (2011). Bacterial subversion of host actin dynamics at the plasma membrane. *Cell. Microbiol.* 13, 1460–1469. doi: 10.1111/j.1462-5822.2011.01651.x

Carlson, S. A., Omary, M. B., and Jones, B. D. (2002). Identification of cytokeratins as accessory mediators of Salmonella entry into eukaryotic cells. *Life Sci.* 70, 1415–1426. doi: 10.1016/S0024-3205(01)01512-0

Caulin, C., Ware, C. F., Magin, T. M., and Oshima, R. G. (2000). Keratin-dependent, epithelial resistance to tumor necrosis factor-induced apoptosis. *J. Cell Biol.* 149, 17–22. doi: 10.1083/jcb.149.1.17

Chan, J. K. L., Yuen, D., Too, P. H. M., Sun, Y., Willard, B., Man, D., et al. (2018). Keratin 6a reorganization for ubiquitin-proteasomal processing is a direct antimicrobial response. *J. Cell Biol.* 217, 731–744. doi: 10.1083/jcb.201704186

Chen, P. H., Ornelles, D. A., and Shenk, T. (1993). The adenovirus L3 23-kilodalton proteinase cleaves the amino-terminal head domain from cytokeratin 18 and disrupts the cytokeratin network of HeLa cells. *J. Virol.* 67, 3507–3514.

Chung, B. M., Arutyunov, A., Ilagan, E., Yao, N., Wills-Karp, M., and Coulombe, P. A. (2015). Regulation of C-X-C chemokine gene expression by keratin 17 and hnRNP K in skin tumor keratinocytes. *J. Cell Biol.* 208, 613–627. doi: 10.1083/jcb.201408026

Claser, C., Curcio, M., Mello, S. M., de, Silveira, E. V., Monteiro, H. P., and Rodrigues, M. M. (2008). Silencing cytokeratin 18 gene inhibits intracellular replication of *Trypanosoma cruzi* in HeLa cells but not binding and invasion of trypanosomes. *BMC Cell Biol.* 9:68. doi: 10.1186/1471-2121-9-68

Colonne, P. M., Winchell, C. G., and Voth, D. E. (2016). Hijacking host cell highways: manipulation of the host actin cytoskeleton by obligate intracellular bacterial pathogens. *Front. Cell. Infect. Microbiol.* 6:107. doi: 10.3389/fcimb.2016.00107

Copp, J., Marino, M., Banerjee, M., Ghosh, P., and van der Geer, P. (2003). Multiple regions of internalin B contribute to its ability to turn on the Ras-mitogen-activated protein kinase pathway. *J. Biol. Chem.* 278, 7783–7789. doi: 10.1074/jbc.M211666200

Czuczman, M. A., Fattouh, R., van Rijn, J. M., Canadien, V., Osborne, S., Muise, A. M., et al. (2014). *Listeria monocytogenes* exploits efferocytosis to promote cell-to-cell spread. *Nature* 509, 230–234. doi: 10.1038/nature13168

Duan, Y., Sun, Y., Zhang, F., Zhang, W. K., Wang, D., Wang, Y., et al. (2012). Keratin K18 increases cystic fibrosis transmembrane conductance regulator (CFTR) surface expression by binding to its C-terminal hydrophobic patch. *J. Biol. Chem.* 287, 40547–40559. doi: 10.1074/jbc.M112.403584

Egile, C., Loisel, T. P., Laurent, V., Li, R., Pantaloni, D., Sansonetti, P. J., et al. (1999). Activation of the CDC42 effector N-WASP by the *Shigella flexneri* IcsA protein promotes actin nucleation by Arp2/3 complex and bacterial actin-based motility. *J. Cell Biol.* 146, 1319–1332. doi: 10.1083/jcb.146.6.1319

Eriksson, J. E., Dechat, T., Grin, B., Helfand, B., Mendez, M., Pallari, H., et al. (2009). Introducing intermediate filaments: from discovery to disease. *J. Clin. Invest.* 119, 1763–1771. doi: 10.1172/JCI38339

Escobar-Hoyos, L. F., Shah, R., Roa-Pena, L., Vanner, E. A., Najafian, N., Banach, A., et al. (2015). Keratin-17 promotes p27KIP1 nuclear export and degradation and offers potential prognostic utility. *Cancer Res.* 75, 3650–3662. doi: 10.1158/0008-5472.CAN-15-0293

Esue, O., Carson, A. A., Tseng, Y., and Wirtz, D. (2006). A direct interaction between actin and vimentin filaments mediated by the tail domain of vimentin. *J. Biol. Chem.* 281, 30393–30399. doi: 10.1074/jbc.M605452200

Felkl, M., Tomas, K., Smid, M., Mattes, J., Windoffer, R., and Leube, R. E. (2012). Monitoring the cytoskeletal EGF response in live gastric carcinoma cells. *PLoS ONE* 7:e45280. doi: 10.1371/journal.pone.0045280

Freitag, N., Port, G., and Miner, M. (2009). *Listeria monocytogenes*—from saprophyte to intracellular pathogen. *Nat. Rev. Microbiol.* 7, 623–628. doi: 10.1038/nrmicro2171

Galarneau, L., Loranger, A., Gilbert, S., and Marceau, N. (2007). Keratins modulate hepatic cell adhesion, size and G1/S transition. *Exp. Cell Res.* 313, 179–194. doi: 10.1016/j.yexcr.2006.10.007

Geisler, F., and Leube, R. E. (2016). Epithelial intermediate filaments: guardians against microbial infection? *Cells* 5, 1–18. doi: 10.3390/cells5030029.

Gessain, G., Tsai, Y.-H., Travier, L., Bonazzi, M., Grayo, S., Cossart, P., et al. (2015). PI3-kinase activation is critical for host barrier permissiveness to *Listeria monocytogenes*. *J. Exp. Med.* 212, 165–183. doi: 10.1084/jem.20141406

Gilbert, S., Loranger, A., Daigle, N., and Marceau, N. (2001). Simple epithelium keratins 8 and 18 provide resistance to Fas-mediated apoptosis. The protection occurs through a receptor-targeting modulation. *J. Cell Biol.* 154, 763–773. doi: 10.1083/jcb.200102130

Gilbert, S., Loranger, A., Lavoie, J. N., and Marceau, N. (2012). Cytoskeleton keratin regulation of FasR signaling through modulation of actin/ezrin interplay at lipid rafts in hepatocytes. *Apoptosis* 17, 880–894. doi: 10.1007/s10495-012-0733-2

Gilbert, S., Loranger, A., Omary, M. B., and Marceau, N. (2016). Keratin impact on PKCδ- and ASMase-mediated regulation of hepatocyte lipid raft size - implication for FasR-associated apoptosis. *J. Cell Sci.* 129, 3262–3273. doi: 10.1242/jcs.171124

Goldman, R. D., Cleland, M. M., Murthy, S. N. P., Mahammad, S., and Kuczmarski, E. R. (2012). Inroads into the structure and function of intermediate filament networks. *J. Struct. Biol.* 177, 14–23. doi: 10.1016/j.jsb.2011.11.017

González, A., Shimobayashi, M., Eisenberg, T., Merle, D. A., Pendl, T., Hall, M. N., et al. (2015). TORC1 promotes phosphorylation of ribosomal protein S6 via the AGC kinase Ypk3 in *Saccharomyces cerevisiae*. *PLoS ONE* 10:e0120250. doi: 10.1371/journal.pone.0120250

Goosney, D. L., Gruenheid, S., and Finlay, B. B. (2000). Gut feelings: enteropathogenic *E. coli* (EPEC) interactions with the host. *Annu. Rev. Cell Dev. Biol.* 16, 173–189. doi: 10.1146/annurev.cellbio.16.1.173

Gruenheid, S., DeVinney, R., Bladt, F., Goosney, D., Gelkop, S., Gish, G. D., et al. (2001). Enteropathogenic, *E. coli* Tir binds Nck to initiate actin pedestal formation in host cells. *Nat. Cell Biol.* 3, 856–859. doi: 10.1038/ncb0901-856

Habtezion, A., Toivola, D. M., Asghar, M. N., Kronmal, G. S., Brooks, J. D., Butcher, E. C., et al. (2011). Absence of keratin 8 confers a paradoxical microflora-dependent resistance to apoptosis in the colon. *Proc. Natl. Acad. Sci. U.S.A.* 108, 1445–1450. doi: 10.1073/pnas.1010833108

Haglund, C. M., and Welch, M. D. (2011). Pathogens and polymers: microbe-host interactions illuminate the cytoskeleton. *J. Cell Biol.* 195, 7–17. doi: 10.1083/jcb.201103148

Haines, R. L., and Lane, E. B. (2012). Keratins and disease at a glance. *J. Cell Sci.* 125, 3923–3928. doi: 10.1242/jcs.099655

Havugimana, P. C., Hart, G. T., Nepusz, T., Yang, H., Turinsky, A. L., Li, Z., et al. (2012). A census of human soluble protein complexes. *Cell* 150, 1068–1081. doi: 10.1016/j.cell.2012.08.011

He, T., Stepulak, A., Holmström, T. H., Omary, M. B., and Eriksson, J. E. (2002). The intermediate filament protein keratin 8 is a novel cytoplasmic substrate for c-Jun N-terminal kinase. *J. Biol. Chem.* 277, 10767–10774. doi: 10.1074/jbc.M111436200

Heinzen, R. A., Grieshaber, S. S., Van Kirk, L. S., and Devin, C. J. (1999). Dynamics of actin-based movement by Rickettsia rickettsii in vero cells. *Infect. Immun.* 67, 4201–4207.

Hobbs, R. P., DePianto, D. J., Jacob, J. T., Han, M. C., Chung, B.-M., Batazzi, A. S., et al. (2015). Keratin-dependent regulation of Aire and gene expression in skin tumor keratinocytes. *Nat. Genet.* 47, 933–938. doi: 10.1038/ng.3355

Ireton, K., Payrastre, B., and Cossart, P. (1999). The *Listeria monocytogenes* protein InlB is an agonist of mammalian phosphoinositide 3-kinase. *J. Biol. Chem.* 274, 17025–17032. doi: 10.1074/jbc.274.24.17025

Ireton, K., Payrastre, B., Chap, H., Ogawa, W., Sakaue, H., Kasuga, M., et al. (1996). A role for phosphoinositide 3-kinase in bacterial invasion. *Science* 274, 780–782. doi: 10.1126/science.274.5288.780

Isberg, R. R., and Leong, J. M. (1990). Multiple beta 1 chain integrins are receptors for invasin, a protein that promotes bacterial penetration into mammalian cells. *Cell* 60, 861–871. doi: 10.1016/0092-8674(90)90099-Z

Jiu, Y., Lehtimäki, J., Tojkander, S., Cheng, F., Jäälinoja, H., Liu, X., et al. (2015). Bidirectional interplay between vimentin intermediate filaments and contractile actin stress fibers. *Cell Rep.* 11, 1511–1518. doi: 10.1016/j.celrep.2015.05.008

Karashima, T., Tsuruta, D., Hamada, T., Ishii, N., Ono, F., Hashikawa, K., et al. (2012). Interaction of plectin and intermediate filaments. *J. Dermatol. Sci.* 66, 44–50. doi: 10.1016/j.jdermsci.2012.01.008

Kellner, J. C., and Coulombe, P. A. (2009). Keratins and protein synthesis: the plot thickens. *J. Cell Biol.* 187, 157–159. doi: 10.1083/jcb.200909134

Kim, S., Wong, P., and Coulombe, P. A. (2006). A keratin cytoskeletal protein regulates protein synthesis and epithelial cell growth. *Nature* 441, 362–365. doi: 10.1038/nature04659

Kölsch, A., Windoffer, R., and Leube, R. E. (2009). Actin-dependent dynamics of keratin filament precursors. *Cell Motil. Cytoskeleton* 66, 976–985. doi: 10.1002/cm.20395

Kuehl, C. J., Dragoi, A.-M., Talman, A., and Agaisse, H. (2015). Bacterial spread from cell to cell: beyond actin-based motility. *Trends Microbiol.* 23, 558–566. doi: 10.1016/j.tim.2015.04.010

Kumar, V., Behr, M., Kiritsi, D., Scheffschick, A., Grahnert, A., Homberg, M., et al. (2016). Keratin-dependent thymic stromal lymphopoietin expression suggests a link between skin blistering and atopic disease. *J. Allergy Clin. Immunol.* 138, 1461–1464.e6. doi: 10.1016/j.jaci.2016.04.046

Kumar, V., Bouameur, J.-E., Bär, J., Rice, R. H., Hornig-Do, H.-T., Roop, D. R., et al. (2015). A keratin scaffold regulates epidermal barrier formation, mitochondrial lipid composition, and activity. *J. Cell Biol.* 211, 1057–1075. doi: 10.1083/jcb.201404147

Kumeta, M., Hirai, Y., Yoshimura, S. H., Horigome, T., and Takeyasu, K. (2013). Antibody-based analysis reveals "filamentous vs. non-filamentous" and "cytoplasmic vs. nuclear" crosstalk of cytoskeletal proteins. *Exp. Cell Res.* 319, 3226–3237. doi: 10.1016/j.yexcr.2013.07.021

Lähdeniemi, I. A. K., Misiorek, J. O., Antila, C. J. M., Landor, S. K.-J., Stenvall, C.-G. A., Fortelius, L. E., et al. (2017). Keratins regulate colonic epithelial cell differentiation through the Notch1 signalling pathway. *Cell Death Differ.* 24, 984–996. doi: 10.1038/cdd.2017.28

Li, N., Xiang, G.-S. S., Dokainish, H., Ireton, K., and Elferink, L. A. (2005). The Listeria protein internalin B mimics hepatocyte growth factor-induced receptor trafficking. *Traffic* 6, 459–473. doi: 10.1111/j.1600-0854.2005.00290.x

Loschke, F., Seltmann, K., Bouameur, J., and Magin, T. M. (2015). Regulation of keratin network organization. *Curr. Opin. Cell Biol.* 32, 56–64. doi: 10.1016/j.ceb.2014.12.006

Magnuson, B., Ekim, B., and Fingar, D. C. (2012). Regulation and function of ribosomal protein S6 kinase (S6K) within mTOR signalling networks. *Biochem. J.* 441, 1–21. doi: 10.1042/BJ20110892

Martins, M., Custodio, R., Camejo, A., Almeida, M. T., Cabanes, D., and Sousa, S. (2012). *Listeria monocytogenes* triggers the cell surface expression of Gp96 protein and interacts with its N terminus to support cellular infection. *J. Biol. Chem.* 287, 43083–43093. doi: 10.1074/jbc.M112.422568

Matsui, H., Asou, H., and Inaba, T. (2007). Cytokines direct the regulation of Bim mRNA stability by heat-shock cognate protein 70. *Mol. Cell* 25, 99–112. doi: 10.1016/j.molcel.2006.12.007

Mengaud, J., Ohayon, H., Gounon, P., Mege, R.-M., and Cossart, P. (1996). E-cadherin is the receptor for internalin, a surface protein required for entry of *L. monocytogenes* into epithelial cells. *Cell* 84, 923–932. doi: 10.1016/S0092-8674(00)81070-3

Menko, A. S., Bleaken, B. M., Libowitz, A. A., Zhang, L., Stepp, M. A., and Walker, J. L. (2014). A central role for vimentin in regulating repair function during healing of the lens epithelium. *Mol. Biol. Cell* 25, 776–790. doi: 10.1091/mbc.E12-12-0900

Moll, R., Divo, M., and Langbein, L. (2008). The human keratins: biology and pathology. *Histochem. Cell Biol.* 129, 705–733. doi: 10.1007/s00418-008-0435-6

Mounier, J., Ryter, A., Coquis-Rondon, M., and Sansonetti, P. J. (1990). Intracellular and cell-to-cell spread of *Listeria monocytogenes* involves interaction with F-actin in the enterocytelike cell line Caco-2. *Infect. Immun.* 58, 1048–1058.

Nava-Acosta, R., and Navarro-Garcia, F. (2013). Cytokeratin 8 is an epithelial cell receptor for Pet, a cytotoxic serine protease autotransporter of Enterobacteriaceae. *MBio* 4, e00838–e00813. doi: 10.1128/mBio.00838-13

Pallari, H.-M., and Eriksson, J. E. (2006). Intermediate filaments as signaling platforms. *Sci. STKE* 2006:pe53. doi: 10.1126/stke.3662006pe53

Pan, X., Hobbs, R. P., and Coulombe, P. A. (2012). The expanding significance of keratin intermediate filaments in normal and diseased epithelia. *Curr. Opin. Cell Biol.* 25, 47–56. doi: 10.1016/j.ceb.2012.10.018

Pizarro-Cerdá, J., and Cossart, P. (2009). *Listeria monocytogenes* membrane trafficking and lifestyle: the exception or the rule? *Annu. Rev. Cell Dev. Biol.* 25, 649–670. doi: 10.1146/annurev.cellbio.042308.113331

Pizarro-Cerdá, J., Jonquières, R., Gouin, E., Vandekerckhove, J., Garin, J., and Cossart, P. (2002). Distinct protein patterns associated with *Listeria monocytogenes* InlA- or InlB-phagosomes. *Cell. Microbiol.* 4, 101–115. doi: 10.1046/j.1462-5822.2002.00169.x

Pizarro-Cerdá, J., Kühbacher, A., and Cossart, P. (2012). Entry of *Listeria monocytogenes* in mammalian epithelial cells: an updated view. *Cold Spring Harb. Perspect. Med.* 2:a010009. doi: 10.1101/cshperspect.a010009

Reches, A., Nachmani, D., Berhani, O., Duev-Cohen, A., Shreibman, D., Ophir, Y., et al. (2016). HNRNPR regulates the expression of classical and nonclassical MHC class I proteins. *J. Immunol.* 196, 4967–4976. doi: 10.4049/jimmunol.1501550

Reis, O., Sousa, S., Camejo, A., Villiers, V., Gouin, E., Cossart, P., et al. (2010). LapB, a novel *Listeria monocytogenes* LPXTG surface adhesin, required for entry into eukaryotic cells and virulence. *J. Infect. Dis.* 202, 551–562. doi: 10.1086/654880

Robertson, H., Langdon, W. Y., Thien, C. B., and Bowtell, D. D. (1997). A c-Cbl yeast two hybrid screen reveals interactions with 14-3-3 isoforms and cytoskeletal components. *Biochem. Biophys. Res. Commun.* 240, 46–50. doi: 10.1006/bbrc.1997.7608

Rolhion, N., and Cossart, P. (2017). How the study of *Listeria monocytogenes* has led to new concepts in biology. *Future Microbiol.* 12, 621–638. doi: 10.2217/fmb-2016-0221

Russo, B. C., Stamm, L. M., Raaben, M., Kim, C. M., Kahoud, E., Robinson, L. R., et al. (2016). Intermediate filaments enable pathogen docking to trigger type 3 effector translocation. *Nat. Microbiol.* 1:16025. doi: 10.1038/nmicrobiol.2016.25

Savijoki, K., Alvesalo, J., Vuorela, P., Leinonen, M., and Kalkkinen, N. (2008). Proteomic analysis of *Chlamydia pneumoniae*-infected HL cells reveals extensive degradation of cytoskeletal proteins. *FEMS Immunol. Med. Microbiol.* 54, 375–384. doi: 10.1111/j.1574-695X.2008.00488.x

Seipelt, J., Liebig, H. D., Sommergruber, W., Gerner, C., and Kuechler, E. (2000). 2A proteinase of human rhinovirus cleaves cytokeratin 8 in infected HeLa cells. *J. Biol. Chem.* 275, 20084–20089. doi: 10.1074/jbc.275.26.20084

Seveau, S., Bierne, H., Giroux, S., Prévost, M.-C., and Cossart, P. (2004). Role of lipid rafts in E-cadherin– and HGF-R/Met–mediated entry of *Listeria monocytogenes* into host cells. *J. Cell Biol.* 166, 743–753. doi: 10.1083/jcb.200406078

Shen, Y., Naujokas, M., Park, M., and Ireton, K. (2000). InIB-dependent internalization of Listeria is mediated by the Met receptor tyrosine kinase. *Cell* 103, 501–510. doi: 10.1016/S0092-8674(00)00141-0

Sousa, S., Cabanes, D., Bougnères, L., Lecuit, M., Sansonetti, P., Tran-Van-Nhieu, G., et al. (2007). Src, cortactin and Arp2/3 complex are required for E-cadherin-mediated internalization of Listeria into cells. *Cell. Microbiol.* 9, 2629–2643. doi: 10.1111/j.1462-5822.2007.00984.x

Sousa, S., Cabanes, D., El-Amraoui, A., Petit, C., Lecuit, M., and Cossart, P. (2004). Unconventional myosin VIIa and vezatin, two proteins crucial for Listeria entry into epithelial cells. *J. Cell Sci.* 117, 2121–2130. doi: 10.1242/jcs.01066

Souza Santos, M., and Orth, K. (2015). Subversion of the cytoskeleton by intracellular bacteria: lessons from Listeria, Salmonella and Vibrio. *Cell. Microbiol.* 17, 164–173. doi: 10.1111/cmi.12399

Stone, M. R., O'Neill, A., Catino, D., and Bloch, R. J. (2005). Specific interaction of the actin-binding domain of dystrophin with intermediate filaments containing keratin 19. *Mol. Biol. Cell* 16, 4280–4293. doi: 10.1091/mbc.E05-02-0112

Stradal, T. E., and Costa, S. C. (2017). Type III secreted virulence factors manipulating signaling to Actin dynamics. *Curr. Top. Microbiol. Immunol.* 399, 175–199. doi: 10.1007/82_2016_35

Swaminathan, B., and Gerner-Smidt, P. (2007). The epidemiology of human listeriosis. *Microbes Infect.* 9, 1236–1243. doi: 10.1016/j.micinf.2007.05.011

Tang, P., Sutherland, C. L., Gold, M. R., and Finlay, B. B. (1998). *Listeria monocytogenes* invasion of epithelial cells requires the MEK-1/ERK-2 mitogen-activated protein kinase pathway. *Infect. Immun.* 66, 1106–1112.

Toivola, D. M., Strnad, P., Habtezion, A., and Omary, M. B. (2010). Intermediate filaments take the heat as stress proteins. *Trends Cell Biol.* 20, 79–91. doi: 10.1016/j.tcb.2009.11.004

Valencia-Gallardo, C. M., Carayol, N., and Tran Van Nhieu, G. (2015). Cytoskeletal mechanics during Shigella invasion and dissemination in epithelial cells. *Cell. Microbiol.* 17, 174–182. doi: 10.1111/cmi.12400

Vanhaesebroeck, B., Stephens, L., and Hawkins, P. (2012). PI3K signalling: the path to discovery and understanding. *Nat. Rev. Mol. Cell Biol.* 13, 195–203. doi: 10.1038/nrm3290

Vijayaraj, P., Kröger, C., Reuter, U., Windoffer, R., Leube, R. E., and Magin, T. M. (2009). Keratins regulate protein biosynthesis through localization of GLUT1 and −3 upstream of AMP kinase and Raptor. *J. Cell Biol.* 187, 175–184. doi: 10.1083/jcb.200906094

Welch, M. D., Iwamatsu, A., and Mitchison, T. J. (1997). Actin polymerization is induced by Arp2/3 protein complex at the surface of *Listeria monocytogenes*. *Nature* 385, 265–269. doi: 10.1038/385265a0

Windoffer, R., Kölsch, A., Wöll, S., and Leube, R. E. (2006). Focal adhesions are hotspots for keratin filament precursor formation. *J. Cell Biol.* 173, 341–348. doi: 10.1083/jcb.200511124

Wu, X., and Brewer, G. (2012). The regulation of mRNA stability in mammalian cells: 2.0. *Gene* 500, 10–21. doi: 10.1016/j.gene.2012.03.021

Yarosh, C. A., Iacona, J. R., Lutz, C. S., and Lynch, K. W. (2015). PSF: Nuclear busy-body or nuclear facilitator? *Wiley Interdiscip. Rev. RNA* 6, 351–367. doi: 10.1002/wrna.1280

Conflict of Interest Statement: The authors declare that the research was conducted in the absence of any commercial or financial relationships that could be construed as a potential conflict of interest.

Copyright © 2018 Cruz, Pereira-Castro, Almeida, Moreira, Cabanes and Sousa. This is an open-access article distributed under the terms of the Creative Commons Attribution License (CC BY). The use, distribution or reproduction in other forums is permitted, provided the original author(s) and the copyright owner are credited and that the original publication in this journal is cited, in accordance with accepted academic practice. No use, distribution or reproduction is permitted which does not comply with these terms.